Ontario Hydro

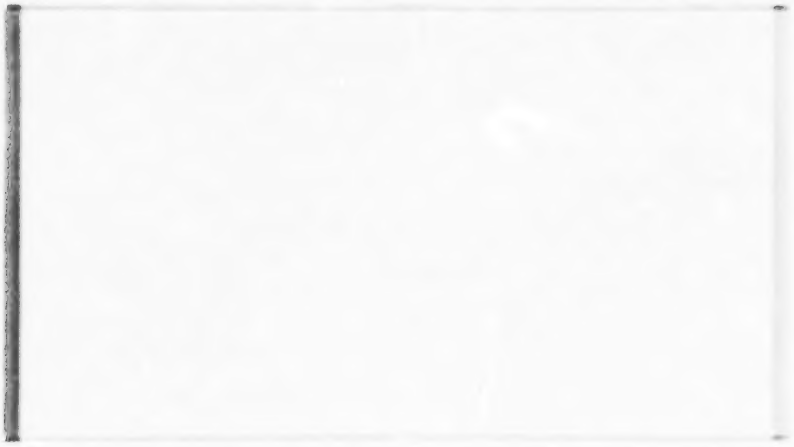

RESEARCH DIVISION

91602
new 82-10

ontario hydro
research division

GAS-METAL-ARC WELDING STUDIES FOR THE FINAL CLOSURE OF COPPER NUCLEAR FUEL WASTE DISPOSAL CONTAINERS

Report No 86-35-K

J.G. Galloway and P.Y.Y. Maak
Technician Engineer
Metallurgy Section
Metallurgical Research Department

ABSTRACT

It has been demonstrated that sound single-vee-groove butt joints can be made in 25-mm-thick electrolytic tough pitch copper using gas metal arc welding. This appears to be a feasible process for the final closure of copper nuclear fuel waste disposal containers. The effects of preheat, heat input, current density and joint restraint on weld quality and mechanical properties of copper gas metal arc welds are described.

job	file	date	report no.
81-144-461	823.241	January 14, 1987	86-35-K

91602
new 82-10

ontario hydro
research division

EXECUTIVE SUMMARY

GAS-METAL-ARC WELDING STUDIES FOR THE FINAL CLOSURE OF COPPER NUCLEAR FUEL WASTE DISPOSAL CONTAINERS

J.G. Galloway and P.Y.Y. Maak
Metallurgy Section
Metallurgical Research Department

As part of Ontario Hydro's technical assistance to the Canadian Nuclear Fuel Waste Management Program, the Welding Unit of the Metallurgical Research Department is investigating the feasibility of using gas-metal-arc welding for the final closure of copper containers for nuclear fuel waste disposal.

We have shown in the present work that single-vee-groove, gas-metal-arc welds containing no gross defects can be made in 25-mm thick electrolytic tough pitch copper in the flat (1G) welding position. High welding current ($\geq$800 A) or high heat input, in conjunction with the use of large-diameter electrode wire (3.2-mm), appeared to produce hot cracking in the copper welds, particularly when high restraint was imposed on the weld joint. In comparison, smaller diameter (1.6- and 2.4-mm) electrode wires were more suitable for welding thick copper. Higher current densities can be obtained, which produce better fusion characteristics with a relatively lower heat input. For the 1.6-mm and 2.4-mm wire, the most suitable ranges of welding current and preheat were found to be from 500 to 600 A and 400^{o} to 500^{o}C, respectively. Excessive preheat ($\geq$600^{o}C) should be avoided as it tends to produce large amounts of gas porosity in the heat-affected zone. The tensile properties of the copper welds were fair. In comparison to the base metal, the weld samples displayed lower tensile strength and ductility.

job	file	date	report no.
81-144-461	823.241	January 14, 1987	86-35-K

TABLE OF CONTENTS

		PAGE
1.0	**INTRODUCTION**	1
2.0	**BEAD-ON-PLATE WELDING STUDIES**	2
2.1	Objectives	2
2.2	Test Materials and Equipment	2
2.3	Experimentation	3
2.4	Experimental Results	3
2.4.1	General Welding Characteristics	3
2.4.2	Weld Deposit Discontinuities	4
2.4.3	Effects of Welding Conditions and Welding Parameters on the Bead Shape and Occurrence of Weld Defects	4
2.4.3.1	Welding Current and Preheat	4
2.4.3.2	Arc Voltage	5
2.4.3.3	Welding Speed and Wire Diameter	6
2.4.3.4	Base Metal	6
2.5	Summary of the Bead-On-Plate Test Results	6
3.0	**GROOVE WELDING TRIALS**	7
3.1	Experimentation	7
3.1.1	Welding Trials	8
3.1.2	Weld Evaluation Techniques	8
3.2	Weld Test Results	8
3.2.1	Metallographic and Radiographic Examination	8
3.2.1.1	General Microstructure	8
3.2.1.2	Welding Trials 14-17 and 22 (3.2 mm diameter wire)	8
3.2.1.3	Welding Trials 41-43 (1.6 mm diameter wire)	9
3.2.1.4	Welding Trials 44-48 (2.4 mm diameter wire)	10
3.2.2	Tensile Tests	10
3.2.3	Hardness Tests	12

TABLE OF CONTENTS (cont'd)

	PAGE
3.3 Discussion of the Groove Weld Test Results	12
3.3.1 Factors Affecting the Formation of Weld Discontinuities in ETP Copper GMA Welds	12
3.3.2 Mechanical Properties of the ETP Copper GMA Welds	12
3.3.3 Temperature Rise of Copper Test Piece During Welding	14
4.0 FUTURE WORK	14
5.0 CONCLUSIONS	15
ACKNOWLEDGEMENT	16
REFERENCES	17
TABLES	18-26
FIGURES	27-46
DISTRIBUTION	last page

LIST OF TABLES

		Page
TABLE I	Chemical Requirements of Copper Used in Procedure Development	18
TABLE II	Fixed Input Welding Parameters	19
TABLE III	Test Parameters and Results of Bead-On-Plate Welding Trials	20
TABLE IV	Copper GMA Groove Welds	23
TABLE V	Tensile Test Results	25

LIST OF FIGURES

Figure 1	Copper GMA Welding Equipment Setup	27
Figure 2	Copper Bead-On-Plate Weld Discontinuities	27
Figure 3	Bead-On-Plate Measurement Definitions	28
Figure 4	Practical Current Range for GMAW (Copper Wires)	29
Figure 5	Current Density vs Welding Current (Calculated)	30
Figure 6	Effects of Welding Current on Bead Shape	31
Figure 7	Effects of Preheat Temperature on Bead Shape	32
Figure 8	Effects of Travel Speed on Bead Shape	33
Figure 9	Joint Designs (Butt Welds)	34
Figure 10	Copper GMA Groove Welding Restraint Jig	35
Figure 11	Macrostructure and Microstructure of a Typical Electrolytic Tough Pitch Copper GMA Weld	36
Figure 12	Cracking Found in Weld 15	37
Figure 13	Weld 22	38
Figure 14	Weld 41	38

LIST OF FIGURES (cont'd)

		Page
Figure 15	Cross-Section and Radiograph of Weld 48 (200°C Preheat)	39
Figure 16	Cross-Section and Radiograph of Weld 44 (500°C Preheat)	40
Figure 17	Cross-Section and Radiograph of Weld 47 (600°C Preheat)	41
Figure 18	Copper Weld Tensile Test Specimens	42
Figure 19	Tensile Test Coupons Showing Fracture at the Weld Metal/Base Metal Interface	43
Figure 20	Cross-Section Through the Fracture Surface of Tensile Test Coupon 47b	43
Figure 21	Tensile Fracture Cross-Section Through Tensile Test Coupon 44B	44
Figure 22	SEM Fractograph of Tensile Test Coupon 44B (1000X)	44
Figure 23	SEM Fractograph of Tensile Test Coupon 47A (1000X)	45
Figure 24	SEM Fractograph of Tensile Test Coupon 47A (100X)	45
Figure 25	Results from Hardness Testing	46

91601
new 82-10

ontario hydro
research division

Mr. H.N. Isaac
Manager
Nuclear Materials Management
Design and Development - Generation

GAS-METAL-ARC WELDING STUDIES FOR THE FINAL CLOSURE OF COPPER NUCLEAR FUEL WASTE DISPOSAL CONTAINERS

1.0 INTRODUCTION

As part of Ontario Hydro's technical assistance to the Canadian Nuclear Fuel Waste Management Program, the Welding Unit of the Metallurgical Research Department is developing suitable welding procedures for the final closure of nuclear fuel waste disposal containers/1/. Pure copper is one of the candidate container materials being considered. Preliminary designs call for a 19-25 mm thick copper container/2,3/.

Compared to steel, copper not only possesses much higher thermal conductivity, but also greater thermal expansion upon heating, and greater contraction during cooling. Weldments of thick copper are thus generally subjected to a high cooling rate and high thermal stresses during cooling, particularly when substantial restraint is imposed on the weld joint. Previous work has shown that pure copper is susceptible to hot shortness, ie, a marked reduction in tensile strength between 200° and 600°C/4/. High thermal stresses, together with the fall-off in mechanical strength at high temperature, may often lead to hot cracking in both the heat-affected zone and the weld/5/. At greater thickness, a higher current (heat input), in conjunction with higher preheat, is required to avoid lack-of-fusion defects. However, it has been found that the risk of formation of weld defects such as gas porosity, "wormholes" (tunnelling) and hot cracks increases with increasing welding current or heat input/5,6/. It has also been reported that segregation of oxygen to the grain boundaries causes grain boundary decohesion and reduction in tensile ductility/7/. It is generally known that high heat input and high preheat may produce excessive gas porosity and promote oxygen segregation at the grain boundaries in the heat-affected zone. Therefore, careful selection of the welding conditions and parameters are essential to produce defect-free copper welds with satisfactory mechanical properties.

Previous work by Ontario Hydro/8/ showed that sound gas-metal-arc single-vee-groove butt joints could be made in 25 mm thick oxygen-free copper plates using a relatively low welding current (350 A) and a relatively high preheat (590°C). For the final closure of nuclear fuel waste disposal containers, it is desirable to use the lowest possible preheat to avoid overheating the contents of the container. Japanese researchers/9/ have demonstrated that sound single-vee-groove butt joints can be made in 25 mm thick electrolytic tough pitch copper plates using gas-metal-arc welding without preheat with extremely high welding currents (>1000 A). However, these welds were made without weld joint restraint. Research at the Welding Institute of Canada confirmed that gas-metal-arc welding of 25 mm thick copper without preheat would require high currents, in the order of 1000 to 1500 A/10/.

The main objective of the present work was to evaluate the effects of preheat and welding parameters on the quality and mechanical integrity of copper gas-metal-arc welds. In addition, the practical range of welding conditions was to be established to produce sound, defect-free copper welds, particularly under conditions of high weld joint restraint.

2.0 BEAD-ON-PLATE WELDING STUDIES

2.1 Objectives

As part of the copper gas metal arc (GMA) welding procedure development, a series of bead-on-plate welding trials was performed on 25 mm thick copper plates in the flat (1G) position. The main purpose of these trials was to determine the useful range of welding conditions and welding parameters for the development of groove welding procedures. The following information was obtained from the bead-on-plate welding trials:

- suitable combinations of preheat and welding current for welding thick copper,
- the effects of parameter changes on bead shape, weld shape, penetration, and defect rate and type,
- the deposition rate, current density and practical current range for 1.6-mm, 2.4-mm and 3.2-mm diameter copper GMA welding wires.

2.2 Test Materials and Equipment

The majority of the bead-on-plate welding trials were performed on 25-mm thick, hot-rolled electrolytic tough pitch copper plates (ie, UNS 11000 copper). The plates were 300-mm square. For comparison purposes, several tests were performed on

oxygen-free electrolytic copper plates (ie, UNS C10100 copper), in the same thickness. The composition of these copper materials is given in Table I.

The welding power source used was an Arcair TekTran Model 750 (maximum current 850 A), set to a constant voltage mode. The wire feeder was a Linde Model SWM-23 and the welding torch was a water-cooled Linde ST-12. The torch and wire feeder were mounted on a remotely controlled travel carriage. The overall equipment setup is shown in Figure 1.

2.3 Experimentation

A total of 35 bead-on-plate welding trials was carried out using different combinations of welding conditions and welding parameters, which included changes of wire diameter, preheat levels, voltage, current and welding speed. Based on the knowledge obtained from previous work/8/, some input welding parameters were selected and remained unchanged through the test program, including the electrical slope, electrode stickout, torch angle and shielding gas composition (see Table II). For the present work, a constant voltage power source was used for GMA welding, and values of welding current were not directly set. The intended current values were obtained by balancing the wire feed speed with the correct voltage for the particular welding conditions. The details of the bead-on-plate welding trials are shown in Table III.

The weld deposits were approximately 275-mm long, and only the last third of the weld run had reliable parameter settings. Control adjustments and fine tuning took place during the first two-thirds of the weld run. All weld bead deposits were compared based on the last third of each run. Optimization of parameter settings, such as voltage, was done by considering the appearance and sound of the ongoing welding process.

Preheat was applied with an oxy-acetylene torch and was monitored with a temperature-indicating crayon. Plate temperature rise was estimated with a series of these crayons.

Weld bead deposits were evaluated from surface appearance and from cross-sections, which were taken at approximately 50 mm from the end of the weld runs. Typical weld defects observed in the weld deposits are shown in Figure 2. Various measurements were made from these cross-sections (see Figure 3). The results are shown in Table III.

2.4 Experimental Results

2.4.1 General Welding Characteristics

Reference 9 provided a graph in which the wire feed speed is plotted against the welding current (see Figure 4). This graph

provided data for pure copper electrode wire diameters of 1.6, 4.0 and 6.0 mm. The lower limit of useable current for each wire size was determined by the critical current for transition from spray transfer to droplet type transfer with a 50% He/50% Ar shielding gas. The upper limit of useable current for each wire size was determined by the current above which irregular bead shape occurred. The welding data obtained from the present work was plotted on the same graph, as shown in Figure 4. Despite the fact that a 75% He/25% Ar shielding gas was used in the present work, the new data fit very well on the graph produced by the Japanese researchers. As shown in Figure 4, the useable range for wire diameters 1.6, 2.4 and 3.2 mm are:

1.6-mm diameter wire - 200 to 700 A
2.4-mm diameter wire - 300 to 850 A
3.2-mm diameter wire - 470 to 920 A

The current densities for each wire were calculated and plotted against welding current in Figure 5. It is shown that, within the useable current range, much higher current densities can be obtained by using smaller diameter wires.

2.4.2 Weld Deposit Discontinuities

Discontinuities such as large voids, wormholes (tunnelling), gas porosity and unfused overlaps were found in some of the bead-on-plate weld deposits. Typical discontinuities are shown in Figure 2. Voids and tunnelling were found in the lower portion of some of the weld beads. Voids appear as isolated, non-uniform cavities. When these cavities are continuous down the length of the weld run, they are labelled as tunnelling. Some weld deposits displayed cold overlaps of unfused weld metal at the weld toe. Small, scattered round porosity (< 0.1 mm in diameter) were in all bead-on-plate weld deposits. However, very little or no gas porosity was found typically in the heat-affected zone. Larger diameter porosity (0.1 to 1.0 mm) was found occasionally on, or near the top surface and near the weld toe of some weld deposits.

2.4.3 Effects of Welding Conditions and Welding Parameters on Weld Bead Shape and Occurrence of Weld Defects

2.4.3.1 Welding Current and Preheat

The effects of welding current and preheat levels on bead shape and weld discontinuities are given in Table III and illustrated in Figure 6 and Figure 7, respectively.

An increase of welding current appeared to have the general effect of increasing the weld bead width (W), weld penetration (P), total weld area (At), and the ratio of fused area to

deposited area (Af/Ad). The effects of welding current on bead height (H) and bead deposit angle (BA) were not clear, as they appeared to be greatly influenced by the preheat level used.

As the plate preheat was increased, the following general effects were observed:

- an increase in weld width (W)
- an increase in weld penetration depth (P)
- an increase in total weld area (At)
- an increase in the ratio of fused area to deposited area (Af/Ad)
- a decrease in reinforcement height (H)
- a decrease in bead angle (BA)

The results showed that high welding current (>800 A) produces large voids, tunnels and overlaps of unfused weld metal, when no or relatively low preheat (<300°C) is used. At higher preheat levels (>300°C), sound bead-on-plate weld deposits could be produced using welding currents in the range of 400 to 700 A.

Rough estimates of plate temperature rise after completion of each weld run were made using temperature-indicating crayons. The plates used in the present work had an approximate volume of 2300 cm^3 and were placed on a large steel backup plate during welding. Measurements of the plate temperature were taken after a time delay of approximately one minute following the weld run, which allowed the plate temperature to become uniform. It was found that with low preheats (20 to 200°C), the plate temperature increased approximately 50° to 70°C. With higher preheats (300° to 600° C), the temperature rise was 0 to 30°C.

2.4.3.2 Arc Voltage

As previously described, the arc voltage was manually adjusted to an apparent optimum value for each set of welding parameters. The present work shows that an increase of arc voltage above the optimum value would have the following effects:

- an increase of weld bead width (W)
- a decrease of weld penetration depth (P)
- a decrease of weld height (H)

These effects were reversed when the arc voltage was decreased below the optimum value. The effect of varying the arc voltage on the Af/Ad ratio was not clear. We also observed that when the arc voltage was raised or lowered from the optimum value, the welding arc became erratic and the bead appearance became rough.

2.4.3.3 Welding Speed and Wire Diameter

The effects of welding speed and wire diameter on weld bead geometry and on the occurrence of weld discontinuities are given in Table III, and are illustrated in Figure 8. The welding speeds used in the present program were 5.0, 6.3 and 7.5 mm/sec, which were within the range of welding speed recommended in Reference 9.

The 3.2-mm diameter wires were tested at room temperature (20°C) with a high current level (600 to 850 A). At relatively low welding speeds of 5.0 and 6.3 mm/sec, the weld appearance was rough and the weld deposit contained large voids and tunnels. Unfused overlaps of weld metal were found. A higher welding speed of 7.5 mm/sec appeared to be necessary to prevent the formation of cold overlaps, but this still produced an excessive bead height and bead deposit angle.

For the 1.6- and 2.4-mm diameter wires, the optimum welding speed was found to be 6.3 mm/sec. These wires were tested at higher preheat (400° to 500°C) and lower current (400 to 500A). Under these testing conditions, all the bead-on-plate test welds were free from weld defects. Variations of welding speed within the range of 5.0 to 7.5 mm/sec produced relatively insignificant changes in weld bead geometry. The results also indicated that the smaller diameter wires produced smaller weld beads with higher Af/Ad ratios. In comparison to the 3.2-mm wire, these small wires produced a smoother bead deposit and a more consistent welding arc.

The limiting factor with the 1.6-mm wire was found to be the inability to feed the wire at a high enough rate to maintain the current above 500 A. It was found that, although the required wire feed speed for currents at, and above 500 A could generally be obtained using the present wire feeder, the wire would periodically bend and jam in the feeding system.

2.4.3.4 Base Metal

Several bead-on-plate test welds were performed on oxygen-free electrolytic (OFE) copper. Under the same welding conditions, no significant difference in bead dimensions and weld quality were found between the ETP and OFE weld deposits.

2.5 Summary of the Bead-on-Plate Test Results

Of all the input test parameters, preheat had the most significant effect on bead geometry and the occurrence of weld discontinuities in the copper bead-on-plate test welds. The results indicated that high preheat (>300°C) was necessary to produce sound welds in 25-mm thick pure copper plates, with no gross defects such as large voids, tunnels and overlaps of unfused weld metal. Furthermore, low preheats tended to produce weld

beads displaying undesirable weld bead geometry (ie, large bead height, large bead deposit angle and small fused area/deposited area ratios), which would likely cause lack-of-fusion defects in multi-pass, copper groove welds.

In comparison with 3.2-mm diameter wire, high current density and better arc stability could be obtained with smaller (1.6- and 2.4-mm) diameter wires. Previous work/9,10/ showed that the intrinsic self-regulation of arc voltage associated with a constant voltage welding machine became sluggish with heavier electrode wire. The instability of the welding arc associated with 3.2-mm diameter wire might be problematic in multi-pass groove welding of thick copper. Better weld bead appearance and desirable bead geometry can be obtained with smaller-diameter wires. The higher current densities associated with the smaller wires appeared to produce better molten metal flow and, hence, better weld metal-to-base metal wetting.

The arc voltage and welding speed also appeared to affect, to a lesser extent, the arc stability, weld bead geometry and the occurrence of weld discontinuities. However, it was shown that suitable welding speed and arc voltage could be determined easily for different sets of welding conditions.

It was shown that the rise of plate temperature above the preheat temperature was quite small (<30°C) when high preheats (300°C to 600°C) were used, suggesting that the maximum temperature attained by the container would depend mainly on the preheat temperature selected for the final closure operation.

3.0 GROOVE WELDING TRIALS

3.1 Experimentation

In conjunction with the bead-on-plate welding tests, single-vee-groove welding trials were performed on 25-mm thick electrolytic tough pitch copper plates. One additional weld (#17) was made on oxygen-free electrolytic copper. The welding equipment and electrode filler wires were the same as those used for bead-on-plate welding trials.

The test plates were 25 x 100 x 300 mm in size. One 300 mm edge of each plate was machined for groove welding. Two weld preparations were used (see Figure 9). In comparison to weld preparation A, weld preparation B had a smaller land (in both width and height). The welding restraint jig and the test piece set up are illustrated in Figure 10. With this jig, all but four of the test welds were highly restrained against angular distortion to simulate actual fabrication conditions.

A large oxygen-acetylene rosebud heating tip was used for preheating. Both the preheat and interpass temperature were monitored with temperature-indicating crayons, and in some cases,

with a thermocouple. The thermocouple output was recorded on a chart recorder to allow measurement of the plate temperature rise during welding.

3.1.1 Welding Trials

A total of thirteen butt joints were made using various combinations of welding parameters. The fixed input welding parameters are listed in Table II; the variable input welding parameters for each weld are shown in Table IV.

3.1.2 Weld Evaluation Techniques

Cross-section samples were taken at approximately 100 mm from the end of the weld and prepared for metallographic examination.

For volumetric inspection of the remaining weld length (excluding approximately 50 mm of the weld start-up), radiographic testing was employed on several welds (welds 44, 45, 46, 47 and 48). The results revealed indications of large voids and porosity in the weld interior. Two exposures were taken of each joint, at 60 degrees and 90 degrees to the plate surface. These provided some indication of the depth location of any discontinuities. The weld caps and backing were removed prior to radiogaphic examination.

3.2 Weld Test Results

3.2.1 Metallographic and Radiographic Examination

3.2.1.1 General Microstructure

Figure 11 shows the microstructure of a typical ETP copper GMA weld. Considerable grain coarsening was found in the heat-affected zone. However, there appeared to be no systematic relationship between the welding conditions/parameters and the heat-affected zone grain size. In comparison to the base metal, a higher level of gas porosity was generally observed in the heat-affected zone (see Figure 11b). The weld deposit exhibited a coarse dendritic structure with large columnar grains (see Figure 11a).

3.2.1.2 Welding Trials with 3.2-mm Diameter Wire

Welding trials 14-17 and 22 were carried out with 3.2-mm diameter wire and a high welding current of 800 A. Relatively low preheats (250° to 350°C) were used. All the welds (except weld 17) were made in ETP copper. Weld 17 was made in OFE copper. The types of weld discontinuities detected in these welds by metallographic examination are shown in Table IV.

All weld cross-sections were free of large voids and tunnels. Small amounts of gas porosity were found in the fused weld metal of all welds. The levels of gas porosity appeared to be higher than those found in the other welds made with smaller diameter wires and lower welding current. Lack-of-fusion defects were found in the cross-sections of all these welds. With the same preheat and welding parameters as weld 16, weld 17, which was made in OFE copper, showed no improvement in the reduction of gas porosity and lack-of-fusion defects.

Welds 14,15,16 and 17 were made without restraint against angular distortion. Weld 15, which was made at the highest preheat (350°C), displayed severe hot cracking, both in the heat-affected zone and in the fused weld metal (see Figure 12). These cracks were found at the grain boundaries in the heat-affected zone and in the interdendritic region in the weld metal.

Weld 22 was made with weld 14 test parameters but with the test pieces clamped into the restraint jig. In contrast to weld 14, weld 22 displayed severe cracking in the heat-affected zone and in the weld metal. Metallographic examination of a cross section of weld 22 (see Figure 13) showed a large crack originating in the heat-affected zone on one side of the joint and propagating through the centre of several weld passes. This crack was visible on the weld surface after completion of the second weld pass and was observed in subsequent weld passes.

These test results appeared to show that large-diameter (3.2-mm) electrode wire in conjunction with the use of high welding current (800 A) tends to produce copper welds containing lack-of-fusion defects and hot cracking, particularly when high restraint and relatively low preheat (350°C) are applied. At 800 A, the heat input level (4.05 kJ/mm) was very high. To reduce the hot cracking tendency, it was imperative that welding current, and thus heat input, be reduced. The susceptibility to lack-of-fusion defects may also be reduced by improving the welding arc stability and increasing the current density. Therefore, the additional weld tests were performed with smaller diameter electrode wire and lower welding currents.

3.2.1.3 Welding Trials with 1.6-mm Diameter Wire

This series of groove welds (welds 41-43) was made using specimen restraint, 1.6-mm diameter filler wire and welding current in the range of 400 to 600 A. In comparison to those welds made at 800 A with 3.2-mm diameter wire, these welds were made at much higher current density (248.8 to 298.5 A/mm^2) and lower heat input (2.06 to 3.28 kJ/mm). Higher preheats (400 to 600°C) were also used.

With the smaller diameter wire and lower current, the welding arc appeared to be more stable compared to the arc produced at 800 A with 3.2-mm wire. Due to the lower current and lower weld metal deposition rate, the bead size of each pass appeared to be considerably smaller. Cross-sections of the welds in this series (except weld 41) showed no defects such as large voids, tunnels, lack-of-fusion or hot cracks (see Table IV). Metallographic examination and tensile testing showed that weld 41 contained a lack-of-fusion defect on the side wall (over the entire length of the weld), which was caused by a failure to maintain the interpass temperature for that particular weld pass (see Figure 14).

3.2.1.4 Welding Trials with 2.4-mm Diameter Wire

Welds 44-48 were made with 2.4-mm diameter filler wire and welding currents of 500 and 600 A. Details of the welding trials are shown in Table IV. The current densities obtained were in the range of 110.4 to 132.5 A/mm^2, which was higher than the current density found with 3.2-mm wire, but considerably lower than with 1.6-mm wire. The heat input levels obtained with the 2.4-mm wire were in the range of 2.78 to 3.43 kJ/mm, which fell between the heat input levels of the 1.6-mm and 3.2-mm wires. For this set of welds, preheat levels studied were in the range of 200° to 600°C.

Welds 48, 46 and 45 were made at preheats of 200°, 300° and 400°C, respectively. The cross-sections of these welds contained large voids and tunnels. Radiographs showed that these discontinuities were prevalent down the entire length of each weld (see Figure 15).

Weld 44, which was made at a higher preheat of 500°C, was free of any weld discontinuities such as large voids or lack-of-fusion defects, and contained only a small amount of gas porosity. A radiograph revealed that the joint was free of any gross weld defects (see Figure 16).

Weld 47 was made at a preheat of 600°C. The cross-section revealed a fairly high concentration of gas porosity in the heat-affected zone and in the weld metal along the fusion line. However, no other weld discontinuities were found. These findings were corroboroated by radiography (see Figure 17). When the 90° and 60° radiographs were compared, the gas porosity was shown to be concentrated along the fusion line.

3.2.2 Tensile Tests

Full-section and reduced-section tensile tests were performed on selected GMA-welded samples and on the ETP copper base metal (see Figure 18). The results are shown in Table V.

The results showed that the yield strength and per cent elongation of the ETP copper base metal were greatly influenced by the orientation of the tensile test coupons with respect to the rolling direction of the plate. Axial test coupons WR1 and WR2 had an average yield strength of 60.2 MPa and an average per cent elongation of 55.5%. In comparison, transverse tensile test coupons AR1 and AR2 displayed a much higher average yield strength of 196.6 MPa and a lower average per cent elongation of 33.6%. The ultimate tensile strengths of the ETP copper test coupons were in the range of 213.7 to 223.4 MPa and there was no significant difference between the axial and traverse test coupons. Both were very ductile.

In this work, all GMA groove welds were deposited parallel to the rolling direction of the test plates. All the welded test coupons (except coupon 44B) failed near the weld metal/base metal interface through the coupon thickness, showing the original weld contour (see Figure 19 and Table V). Test coupon 44B failed in the weld metal. The yield strengths of the welded coupons were in the range of 48.3 to 74.5 MPa, which were comparable to the yield strengths of the axial base metal test coupons but much lower than the yield strength of the transverse base metal test coupons. The ultimate tensile strengths of the welded test coupons were in the range 147.8 to 193.8 MPa, which is approximately 75.5 to 85.5% of the average ultimate tensile strength of the ETP copper base metal. Test coupon 41, which contained a large lack-of-fusion defect on the side wall, displayed the lowest ultimate tensile strength (147.8 MPa) and was excluded. Compared to the ETP copper base metal, the welded test coupons showed a much lower per cent elongation of 14.0 to 19.4%.

Cross-sections through the fracture surface of the test coupons were prepared metallographically and were examined with an optical microscope. All test coupons, except one, appeared to fail in the coarse-grained heat-affected zone at a distance of one to three grains from the weld metal/base metal interface. The fracture appeared to be ductile and indicated no evidence of a brittle intergranular failure mode (see Figure 20). The fracture surface of test coupon 44B, which failed in the weld metal, also appeared to be ductile (see Figure 21). Cracks were found in the interdendritic region. The fracture surfaces of coupons 44B and 47A were examined by scanning electron microscope. Dimples typical of a ductile fracture were found throughout the entire fracture surface (see Figures 22 and 23). No facets or indications of brittle failure were found. Cavities were found in some areas on the fracture surface of coupon 47A, indicating the presence of gas porosity in the fracture regions (see Figure 24).

3.2.3 Hardness Tests

Hardness tests were performed on selected welded samples. Analysis of the data (see Figure 25), failed to reveal any systematic relationship between hardness and location in the weld area, in spite of the very pronounced grain coarsening in the heat-affected zone and the presence of a coarse dendritic structure in the weld metal. In Reference 11 it was suggested that this lack of softening was due to some work hardening in the weld region, offsetting the expected softening due to grain growth. A higher concentration of dissolved oxygen in the heat-affected zone might also contribute to additional hardening in this region.

3.3 Discussion of Groove Welding Test Results

3.3.1 Factors Affecting the Formation of Weld Discontinuities in ETP Copper GMA Welds

This work has shown that a stable welding arc, and sufficiently high current density and preheat were essential for the production of sound gas-metal-arc welds in 25-mm thick ETP copper.

Welding with the 3.2-mm diameter wire at a high welding current (800 A) tended to produce an unstable welding arc and cause lack-of-fusion defects. Moreover, the high welding current, and thus high heat input, caused hot cracking, both in the heat-affected zone and in the weld deposit, particularly when high restraint or high preheat (350°C) were used.

Better arc stability and high welding current densities can be obtained with the use of smaller diameter (1.6- and 2.4-mm) electrode wires and welding currents in the range of 400 to 600 A. Higher current densities appear to produce better molten metal flow into the groove and better wetting to previous weld passes and to the side wall, thereby minimizing lack-of-fusion defects. With higher current densities, sound GMA welds could be made at lower heat input. This reduction in heat input was the most effective means for preventing hot cracking in thick copper weldments.

With 1.6-mm diameter wire, sound GMA groove welds could be made using welding currents from 400 to 500 A and preheats between 400° and 600°C.

Sound copper GMA groove welds could also be made using 2.4-mm wire and a higher welding current of 600 A. Due to the lower current density obtained, a relatively high preheat of 500°C had to be used. Lower preheats at 200°, 300° and 400°C produced lack-of-fusion defects and large voids in the copper welds. Furthermore, when a high welding current of 600 A was used in

conjunction with a high preheat of 600°C, copper welds were produced with a high concentration of gas porosity in the heat-affected zone and in the weld metal.

In comparison to the 2.4-mm wire, the smaller 1.6-mm wire allows the use of lower current and lower preheat for GMA welding of thick ETP copper which, in turn, would reduce the risk of hot cracking and the formation of excessive gas porosity in the heat-affected zone. However, the problem concerning feeding of the 1.6-mm wire at a high rate must be resolved by equipment modification.

3.3.2 Mechanical Properties of the ETP Copper GMA Welds

ETP copper GMA welds appear to exhibit satisfactory tensile properties. The yield strengths of the welded coupons were comparable to the ETP copper base metal, ie, relative to the yield strength in the rolling direction. The ultimate tensile strengths of the welded coupons were about 75 to 89% of the average value of the base metal.

Compared to the base metal, the welded samples displayed much lower per cent elongation over the 51-mm gauge length (14.0 to 19.4%). However, the fracture surface of all welded test coupons appeared to be very ductile and showed no indications of brittle failure. All welds were deposited parallel to the rolling direction of the test plates. It was also shown that the tensile yield strength of the welds was only about 30% of the tensile yield strength of the base metal. During tensile testing, most (and probably all) of the yielding and plastic deformation occurred in the relatively low-strength weld area, particularly in the relatively narrow heat-affected zone. Localized yielding appeared to account for the calculated low values of per cent elongation over the 51-mm gauge length.

During welding of ETP copper, oxygen (originating from dissolved oxygen in the base metal) tends to diffuse from the base metal through the heat-affected zone into the weld pool, as a result of the normal diffusion from areas with lower temperature to areas with high temperature. Oxygen gas that fails to get into the weld pool is trapped in the heat-affected zone as gas porosity. It was shown that in comparison to the base metal and the weld metal, the heat-affected zone of most of the welded samples contained higher gas porosity. As well as reducing the total cross sectional area of the test coupon, gas porosity might speed up the coalescence of cavities as well as initiating and propagating cracks during tensile testing.

Previous work/7/ showed that excessive oxygen segregation or the presence of a continuous film of cuprous oxide at the grain boundaries might cause embrittlement in copper weld joints. In this work, no continuous copper oxide film was found at the grain boundaries in the heat-affected zones. The lack of any

indication of brittle failure on the fracture surface of the tensile test coupons also confirmed that there was no severe oxygen segregation to grain boundaries in the heat-affected zone. However, we also noted that all hot cracks found were present at grain boundaries, where some form of oxygen segregation might have occurred. During tensile testing, the grain boundaries in the heat-affected zone were likely prone to the formation of cavities and cracks. It appears probable that the presence of coarse grains, a higher level of gas porosity and oxygen segregation at the grain boundaries in the heat-affected zone make this region a preferable site for failure during tensile testing.

Although the level of gas porosity and the extent of oxygen segregation can be minimized by using suitable preheat and input weld parameters, the best solution is to reduce the level of dissolved oxygen in the base metal. In comparison to ETP copper, OFE copper contains an extremely low level of dissolved oxygen, and is recommended for copper nuclear fuel waste disposal container designs.

3.3.3 Temperature Rise During Welding

Changes in the test plate temperatures for welding trials 46 and 47 were recorded during welding. The same input welding parameters (except for preheat temperature) were used for these two welding trials. Weld 46 (see Table IV) was conducted at a preheat of 300°C. During each weld pass, the heat gradually built up and the plate temperature rose to approximately 400°-420°C. After each pass was completed, the test plate was allowed to cool to the preheat temperature prior to starting the next weld pass. Welding trial 47 was prepared with a preheat of 600°C. During each weld pass, the plate temperature increased to about 650°-670°C. However, the plate temperature dropped very rapidly after each pass was completed and the arc was extinguished. Additional heating was required to raise the plate temperature back to 600°C. These results show that during the closure welding of copper containers, the temperature of the weld area would likely have to be closely monitored to maintain the preheat temperature.

4.0 FUTURE WORK

In future studies, the welding parameters developed for ETP copper will be applied and refined for OFE copper. The effects of dissolved oxygen in the base metal on weld quality and mechanical properties will be evaluated. Welding trials will also be performed on an OFE copper pipe mockup to simulate a fuel waste container closure-welding process.

5.0 CONCLUSIONS

5.1 Sound gas-metal-arc groove welds can be made in 25-mm thick electrolytic tough pitch copper plates with small-diameter (1.6- and 2.4-mm) wires. A larger diameter (3.2-mm) wire tends to produce an unstable welding arc and lack-of-fusion defects.

5.2 Of the welding parameters studied, preheat appears to have the most significant effect on weld quality. Inadequate preheat may cause lack-of-fusion defects, large voids or tunnels in the weld. Excessive preheat may also cause high gas porosity in the heat-affected zone. The selection of preheat in the range of 400° to 600°C, in conjunction with appropriate welding parameters, is required to produce sound GMA welds in 25 mm thick copper.

5.3 High welding current ($\geq$800 A), and thus high heat input, may increase the tendency for hot cracking in copper GMA welds, particularly when high restraint is imposed on the weld joint. High current densities can be obtained with smaller diameter (1.6- and 2.4-mm) wire, which improves the molten metal flow into the groove as well as wetting to the previous weld passes and the groove walls. Sound copper welds can then be made at relatively low current (500 to 600 A), and thus at lower heat input.

5.4 The tensile properties of the ETP copper GMA welded samples appear to be fair. During tensile testing, most yielding and straining occurred in the relatively low-strength weld area, particularly in the coarse-grained heat-affected zone. Consequently, a relatively low per cent elongation was observed. However, examination of the fracture surface showed no indications of brittle fracture and the copper weld joints were very ductile. It appears that the weld quality and mechanical properties of copper welds can be improved with base plate material containing a lower level of dissolved oxygen. OFE copper is recommended as the base metal for future studies.

6.0 ACKNOWLEDGEMENTS

The authors wish to express their thanks to Ms. S.V. Sandloehken for the SEM fractography and Mr. A. Kalnins and the personnel at Bruce NGS "B" - Quality Control Welding for the radiographic inspection.

Recommended:

W.H.S. Lawson
Supervising Engineer
Metallurgy Section

Submitted:

J.G. Galloway
Technician - Welding
Metallurgy Section

P.Y.Y. Maak
Engineer - Welding
Metallurgy Section

Approved:

J. Brown
Manager
Metallurgical Research Department

JGG/PYYM:mf

Reviewed:

J.A. Chadha
Area Coordinator
AECL Technical Assistance
Program

REFERENCES

1. **Maak, P.Y.Y.**, (December, 1985). "Progress in Welding Studies for Canadian Nuclear Waste Disposal Containers," Ontario Hydro Research Division Report 85-98-K.

2. **Nuttall, K.** and Urbanic, V.F., (1981). "An Assessment of Materials for Nuclear Fuel Immobilization Containers," Atomic Energy of Canada Limited Report, AECL-6440.

3. **Cameron, D.J.**, Crosthwaite, J.L. and Nutall, K., (1983). "The Development of Durable, Man-Made Containers for Fuel Isolation," publ Canadian Metall. Quarterly, Vol 22, No 1, pp 87-101.

4. **Baker, B.H.**, and Jobber, A., (May, 1960). "Practical Aspects of the Welding of Copper by the Gas-Shielded Bare Wire Process," Welding and Metal Fabrication, pp 185-192.

5. **Wegrzyn, J.**, (1968). "Progress in the Welding of Copper," International Institute of Welding 1968 Annual Assembly, Warsaw.

6. **Spiller, K.R.**, and Weld, I., (February, 1970). "Welding Copper by the Gas Shielded Arc Proceses," Metal Construction and British Welding Journal, Vol 2, No 2.

7. **Nieh, T.G.**, and Nix, W.D., (May, 1981). "Embrittlement of Copper Due to Segregation of Oxygen to Grain Boundaries," Metalurgical Transactions, Vol 12A, No 5, May, 1981.

8. **Maak, P.Y.Y.** (1982). "Preliminary Study of Gas Metal Arc Welding of 25 mm Thick Oxygen Free Copper," Ontario Hydro Research Division Report 81-459-K.

9. **Okada, T.**, Toyouka, T., Wakins, Y. and Yamamoto, H., (1979). High Current Mig Welding for Thick Copper Plate Without Preheat," IIW-XII-C-102-79.

10. **KO, K.**, Bryan, B., and Ditschun, A., (1983). "Welding of Copper for Irradiated Nuclear Fuel Disposal Containers," Welding Institute of Canada Report RC-110.

11. **Mosborg, R.J.**, Bohl, R.W., Howland, F.L. and Munse, W.H., (October, 1951). "Tensile Tests and Metallurgical Studies of Welded Copper Joints," Welding Journal, 5195-5285.

TABLE I

CHEMICAL REQUIREMENTS OF COPPER USED IN PROCEDURE DEVELOPMENT

Classification	Composition (wt %)																		
	Cu	O	Zn	Mn	Si	Ni & Co	Al	P	Pb	Cd	S	Hg	Se	Te	Sn	Bi	Sb	As	Fe
UNS C10100 (ASTM B133)	99.99 min	0.0010	0.0001	(A)	-	-	-	0.0003	0.001	0.0001	0.0018	0.0001	0.001 (A)	0.001 (A)	(A)	0.001 (A)	(A)	(A)	-
UNS C11000 (ASTM B133)	99.90 min (incl Ag)	-	-	-	-	-	-	-	-	-	-	-	-	-	-	-	-	-	-
AWS ER Cu (SFA - 5.7)	98.0 min (incl Ag)	-	-	0.5	0.50	(B)	0.01 (B)	0.15	0.02 (B)	-	-	-	-	-	1.0	-	-	-	(B)

NOTES: All values are maximums unless otherwise stated.

(A) The total of these seven elements not to exceed 40 ppm

(B) The total of these elements and all others not listed shall not exceed 0.50

TABLE II

FIXED INPUT WELDING PARAMETERS

(For Bead-on-Plate and Groove Welding Trials)

Shielding Gas Mixture:	75% Helium/25% Argon
Shielding Gas Flowrate:	60 L/min
Torch Angle:	90° to the work (fixed)
Electrical Slope:	4% (0% = constant voltage)
Electrode Stickout:	~20-25 mm (contact tip to work distance)

TABLE III

TEST PARAMETERS AND RESULTS OF BEAD-ON-PLATE WELDING TRIALS

	Test Parameters							Resulting Weld Bead Characteristics (see Figure 3)							
Weld No	Wire Size (mm)	Material	Preheat (^{o}C)	Current (A)	Arc Voltage (V)	Travel Speed (mm/s)	Defects	W (mm)	P (mm)	H (mm)	A_t (mm^2)	A_f (mm^2)	A_d (mm^2)	A_f/A_d	BA (^{o}0)
1	3.2	ETP	20	800	~38	7.5		13.4	3.7	5.7	101.6	36.0	65.6	0.549	68
2	3.2	ETP	20	800	~41	7.5	Voids	15.1	3.1	4.7	95.4	37.6	57.8	0.651	36
3	3.2	ETP	20	800	~38	5.0	Voids, Overlaps	16.0	4.0	6.3	164.0	45.4	118.6	0.383	82
4	3.2	ETP	20	850	~39	7.5	Voids	15.1	6.3	6.3	163.8	57.6	106.2	0.542	80
5	3.2	ETP	20	700	~35	7.5		12.0	4.0	5.4	92.4	32.4	60.0	0.540	75
6	3.2	ETP	20	600	~33	7.5		11.1	2.3	4.8	68.8	16.2	52.6	0.308	72
7	3.2	ETP	20	800	~38	6.3	Voids, Overlaps	16.3	5.1	5.7	147.8	55.0	92.8	0.593	60
8	3.2	ETP	20	800	~35	7.5	Voids	12.3	4.8	6.0	121.8	53.0	68.8	0.770	65
9	3.2	ETP	100	800	~38	7.5	Voids	16.0	4.8	5.1	126.6	51.0	75.6	0.675	50
10	3.2	ETP	200	800	~38	7.5	Voids	17.1	5.4	5.1	135.0	58.6	76.4	0.767	53
11	3.2	ETP	300	800	~38	7.5		19.4	6.3	4.6	155.0	82.4	72.6	1.135	48
12	3.2	ETP	400	800	~38	7.5		24.0	7.1	4.0	180.4	104.4	76.0	1.374	40
13	3.2	ETP	400	600	~33	7.5		16.6	3.1	2.9	61.2	28.6	32.6	0.877	34
18	3.2	OF	20	800	~38	7.5	Lack of Fusion	16.3	2.9	5.1	105.0	34.4	70.6	0.487	55

TABLE III (cont'd)

TEST PARAMETERS AND RESULTS OF BEAD-ON-PLATE WELDING TRIALS

	Test Parameters							Resulting Weld Bead Characteristics (see Figure 3)							
Weld No	Wire Size (mm)	Material	Preheat (^{o}C)	Current (A)	Arc Voltage (V)	Travel Speed (mm/s)	Defects	W (mm)	P (mm)	H (mm)	A_t (mm^2)	A_f (mm^2)	A_d (mm^2)	A_f/A^d	BA (^{o}0)
19	3.2	OF	100	800	~38	7.5	Voids	16.6	4.3	3.7	96.2	42.0	54.2	0.775	55
20	3.2	OF	200	800	~38	7.5	Voids	18.0	4.9	4.3	123.2	56.8	66.4	0.855	45
21	3.2	OF	300	800	~38	7.5	Voids	18.6	4.9	4.4	140.0	70.6	69.4	1.017	44
23	2.4	ETP	400	600	~36	6.3		20.8	4.8	3.1	110.6	70.4	40.2	1.751	30
24	2.4	ETP	400	500	~35	6.3		18.0	3.7	3.7	87.6	39.2	48.4	0.810	35
25	2.4	ETP	400	400	~34	6.3		11.7	1.4	3.7	41.4	11.4	30.0	0.380	40
26	2.4	ETP	400	500	~35	7.5		15.7	4.0	3.7	71.4	34.4	37.0	0.930	36
27	2.4	ETP	400	500	~35	5.0		17.7	3.1	4.3	90.8	30.8	60.0	0.513	45
28	2.4	ETP	500	500	~35	6.3		16.8	2.6	3.4	70.8	28.0	42.8	0.654	30
29	2.4	ETP	500	400	~34	6.3		15.7	2.0	3.7	63.2	21.6	41.6	0.519	35
30	2.4	ETP	300	600	~36	6.3		16.3	6.6	4.3	115.2	59.6	55.6	1.072	46
31	2.4	ETP	300	500	~35	6.3		15.7	2.9	3.4	72.2	28.4	43.8	0.648	37
32	1.6	ETP	400	600	~34.5	6.3		20.0	6.9	3.4	129.2	77.4	51.8	1.494	37

TABLE III (cont'd)

TEST PARAMETERS AND RESULTS OF BEAD-ON-PLATE WELDING TRIALS

	Test Parameters							Resulting Weld Bead Characteristics (see Figure 3)							
Weld No	Wire Size (mm)	Material	Preheat (^{o}C)	Current (A)	Arc Voltage (V)	Travel Speed (mm/s)	Defects	W (mm)	P (mm)	H (mm)	A_t (mm^2)	A_f (mm^2)	A_d (mm^2)	A_f/A_d	BA (^{o})
33	1.6	ETP	400	500	~33.5	6.3		16.9	4.6	3.1	99.2	53.6	45.6	1.175	34
34	1.6	ETP	400	400	~32.5	6.3		13.4	2.3	3.4	51.0	16.4	34.6	0.474	45
35	1.6	ETP	500	500	~33.5	6.3		16.6	5.1	3.4	93.4	50.2	43.2	1.162	42
36	1.6	ETP	500	400	~32.5	6.3		13.4	2.3	3.7	55.2	19.0	36.2	0.525	48
37	1.6	ETP	500	400	~32.5	7.5		12.0	2.6	3.1	45.6	19.2	26.2	0.740	44
38	1.6	ETP	500	400	~32.5	5.0		15.4	2.6	4.0	63.8	22.2	41.6	0.534	41
39	1.6	ETP	600	400	~32.5	6.3		15.1	3.1	3.1	64.6	25.0	39.6	0.631	42
40	1.6	ETP	600	500	~33.5	6.3		18.9	4.9	3.4	107.0	64.0	43.0	1.488	37

*Welds No 14-17, 22, 41-48 were groove welds

TABLE IV

COPPER GMA GROOVE WELDS

Weld No	Restraint Y/N	Preheat °C	Wire Dia (mm)	Root Parameters	Fill Parameters	Heat Input (kJ/mm) per pass	Current Density (A/mm^2) per pass	No. of passes	Mat'l	Joint Design	Radiography	Metallography
14	N	300	3.2	800 A 38 V 7.5 mm/s	Same	4.05	99	9	C11000	A	-	interbead LOF
15	N	350	3.2	800 A 38 V 7.5 mm/s	Same	4.05	99	8	C11000	A	-	interbead LOF sidewall LOF underbead cracking
16	N	250	3.2	800 A 38 V 7.5 mm/s	Same	4.05	99	8	C11000	A	-	interbead LOF
17	N	250	3.2	800 A 38 V 7.5 mm/s	Same	4.05	99	8	C10100	A	-	interbead LOF
22	Y	300	3.2	800 A 38 V 7.5 mm/s	Same	4.05	99	8	C11000	A	-	interbead LOF large cracks
41	Y	600	1.6	500 A 33.5 V 6.3 mm/s	400 A 32.5 V 6.3 mm/s	2.66(R) 2.06(F)	248(R) 198(F)	1(R) 13(F)	C11000	B	-	interbead LOF
42	Y	500	1.6	500 A 33.5 V 6.3 mm/s	Same	2.66	248	13	C11000	B	-	acceptable
43	Y	400	1.6	600 A 34.5 V 6.3 mm/s	500 A 33.5 V 6.3 mm/s	3.28(R) 2.66(F)	298 248	2(R) 7(F)	C11000	B	-	acceptable

TABLE IV (cont'd)

COPPER GMA GROOVE WELDS

Weld No	Restraint Y/N	Preheat °C	Wire Dia (mm)	Root Parameters	Fill Parameters	Heat Input (kJ/mm) per pass	Current Density (A/mm2) per pass	No. of passes	Mat'l	Joint Design	Radiography	Metallography
44	Y	500	2.4	500 A 35 V 6.3 mm/s	600 A 36 V 6.3 mm/s	2.78(R) 3.43(F)	110 (R) 132 (F)	2(R) 7(F)	C11000	B	acceptable	acceptable
45	Y	400	2.4	600 A 36 V 6.3 mm/s	Same	3.43	132	10	C11000	B	large voids	voids
46	Y	300	2.4	500 A 36 V 6.3 mm/s	Same	3.43	132	10	C11000	B	large voids	voids
47	Y	600	2.4	500 A 35 V 6.3 mm/s	600 A 36 V 6.3 mm/s	2.78(R) 3.43(F)	110 (R) 132 (F)	2(R) 7(F)	C11000	B	fusion line porosity	fusion line porosity
48	Y	200	2.4	600A 36 V 6.3 mm/s	Same	3.43	132	10	C11000	B	large voids	interbead LOF sidewall LOF voids

TABLE V

TENSILE TEST RESULTS

Sample No.	Specimen Type	Cross-sectional Area (mm^2)	Breaking Load (kN)	Yield* Strength (MPa)	Ultimate Strength (MPa)	Elongation (2" gauge)	Failure Location	Defects found in Fracture
Weld #41	Full Section	584	86.291	-	147.8	14%	Fusion Line	Lack of Fusion
Weld #43	Full Section	590	114.313	-	193.8	22%	Fusion Line	Porosity
Weld #44A	Round Reduced	131	21.350	48.3	165.5	15.4%	Fusion Line	-
Weld #44B	Round Reduced	129	22.863	54.1	177.2	19.4%	Weld Metal	-
Weld #47A	Round Reduced	130	22.151	74.5	171.6	15.9%	Fusion Line	Fine Porosity
Weld #47B	Round Reduced	128	21.350	60.3	165.5	12.9%	Fusion Line	Porosity
Base WR 1**	Round Reduced	131	28.022	55.8	217.2	58.2%	-	-

TABLE V (cont'd)

TENSILE TEST RESULTS

Sample No.	Specimen Type	Cross-sectional Area (mm^2)	Breaking Load (kH)	Yield* Strength (MPa)	Ultimate Strength (MPa)	Elongation (2" gauge)	Failure Location	Defects found in Fracture
Base WR 2	Round Reduced	129	27.578	64.5	213.7	52.7%	-	-
Base AR 1***	Round Reduced	130	28.645	195.1	222.0	34.8%	-	-
Base AR 2	Round Reduced	131	28.823	198.2	223.4	32.3%	-	-

* Yield Strength taken at 0.1% offset
** Base Metal test with Rolling Direction (WR)
***Base Metal test Across Rolling Direction (AR)

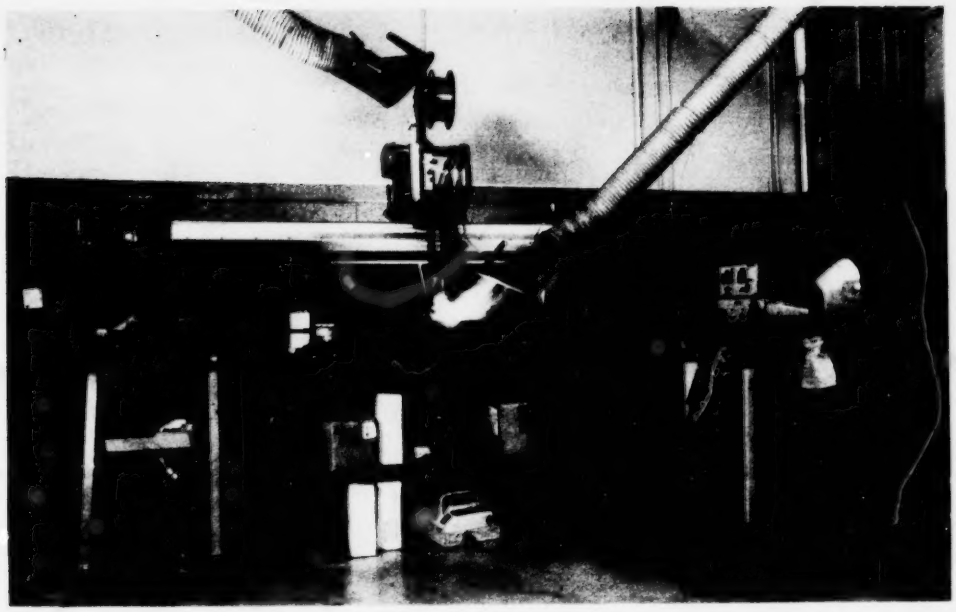

FIGURE 1
COPPER GMA WELDING EQUIPMENT SETUP

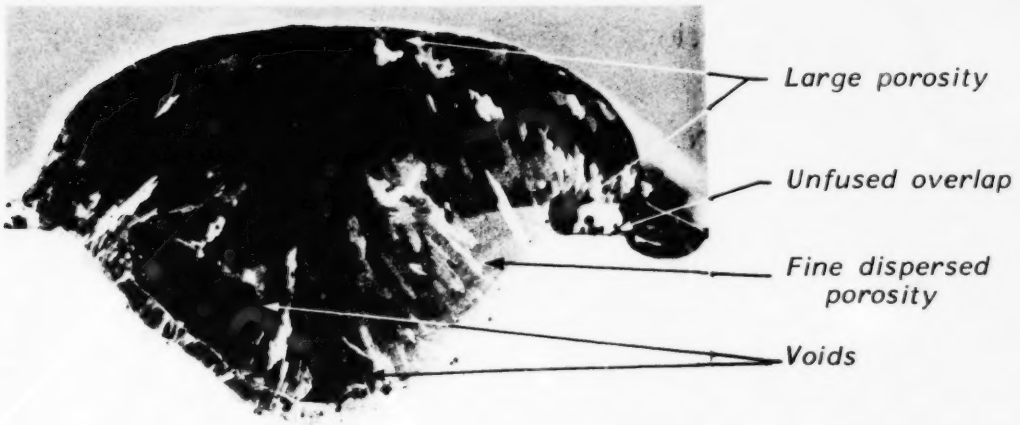

FIGURE 2
COPPER BEAD ON PLATE WELD DISCONTINUITIES
(WELD 4 - 5x)

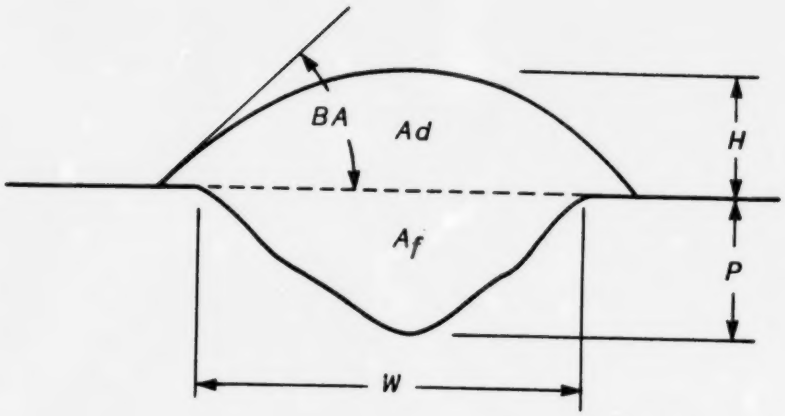

Measured Values:

Ad	=	*Deposited Area (Reinforcement)*
A_f	=	*Fused Area (Base Metal)*
H	=	*Maximum Bead Height*
P	=	*Maximum Depth of Penetration*
W	=	*Bead Width (not including unfused overlaps)*
BA	=	*Bead Deposit Angle (Average of Left & Right Side)*

Calculated Values:

A_t	=	*Total Fused Area (Ad + A_f)*
A_f/Ad	=	*Ratio of Fused Area over Deposited Area*

FIGURE 3

BEAD ON PLATE MEASUREMENT DEFINITIONS

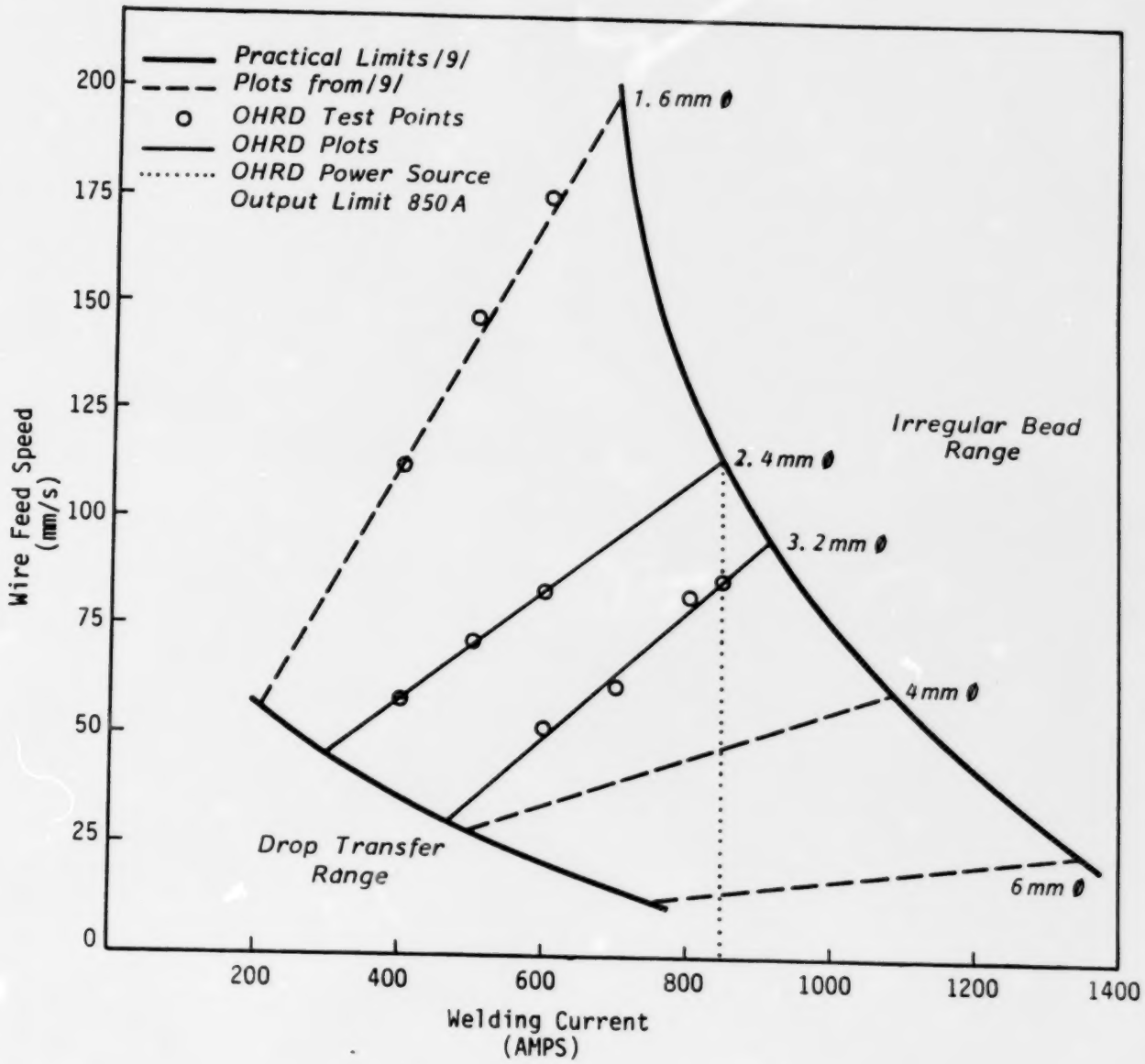

FIGURE 4
PRACTICAL CURRENT RANGE FOR GMAW (COPPER WIRES)

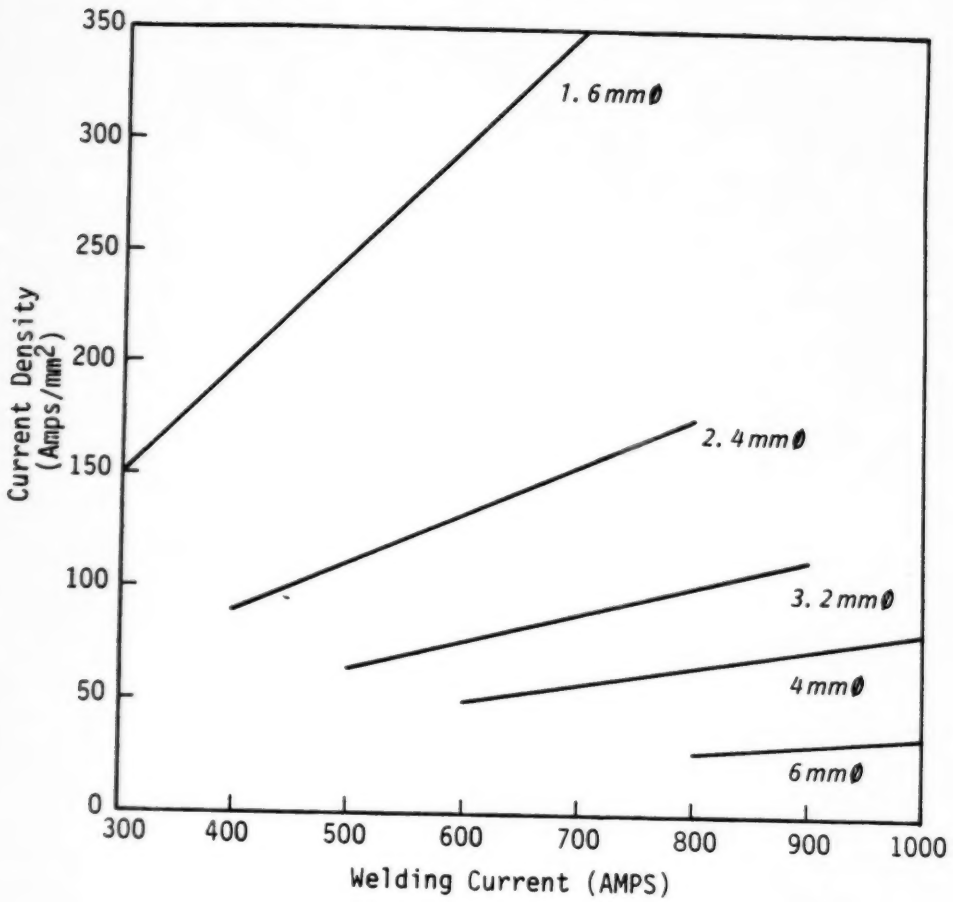

FIGURE 5

CURRENT DENSITY VS WELDING CURRENT
(CALCULATED)

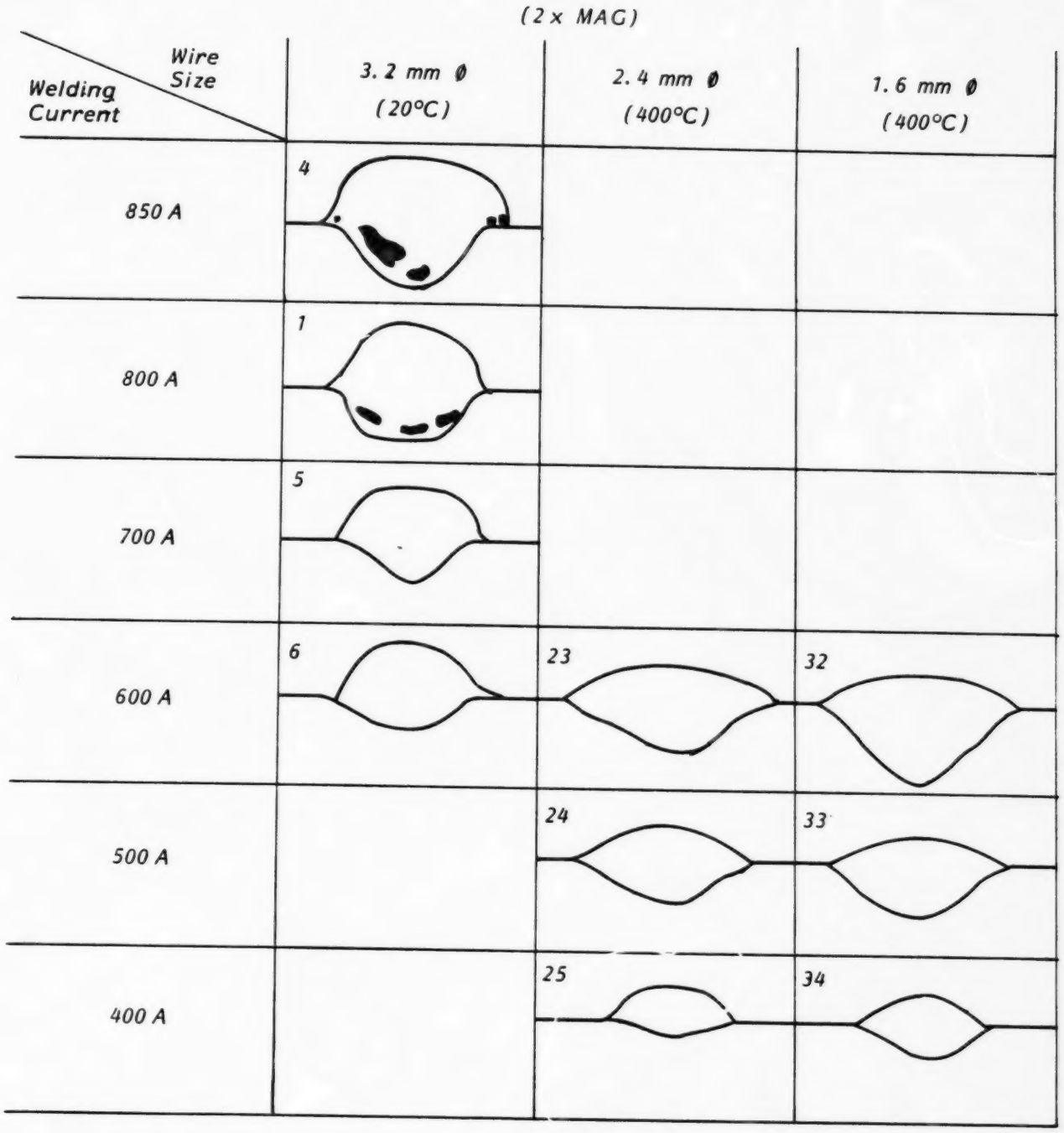

FIGURE 6
EFFECTS OF WELDING CURRENT ON BEAD SHAPE

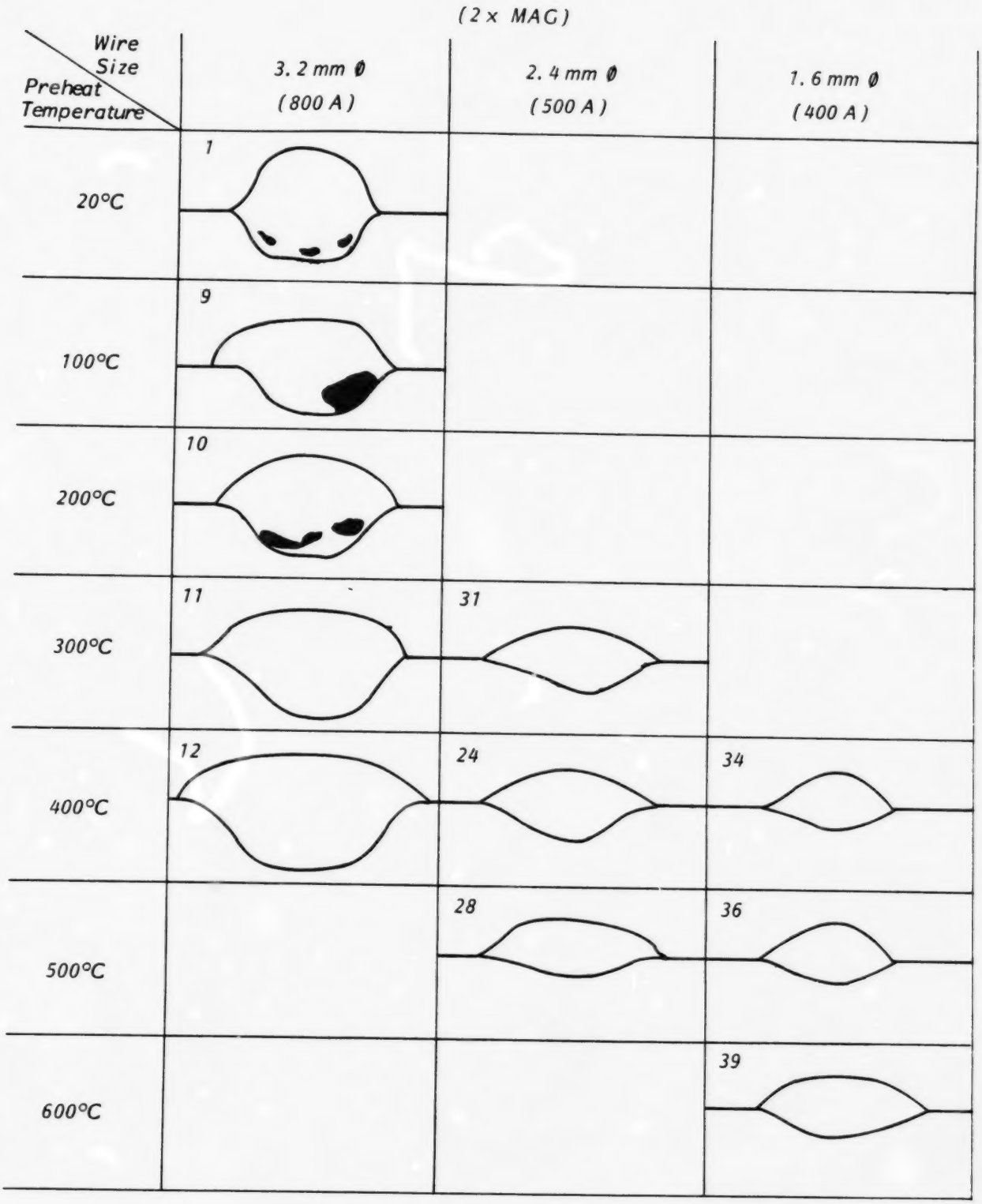

FIGURE 7
EFFECTS OF PREHEAT TEMPERATURE ON BEAD SHAPE

(2x MAG)

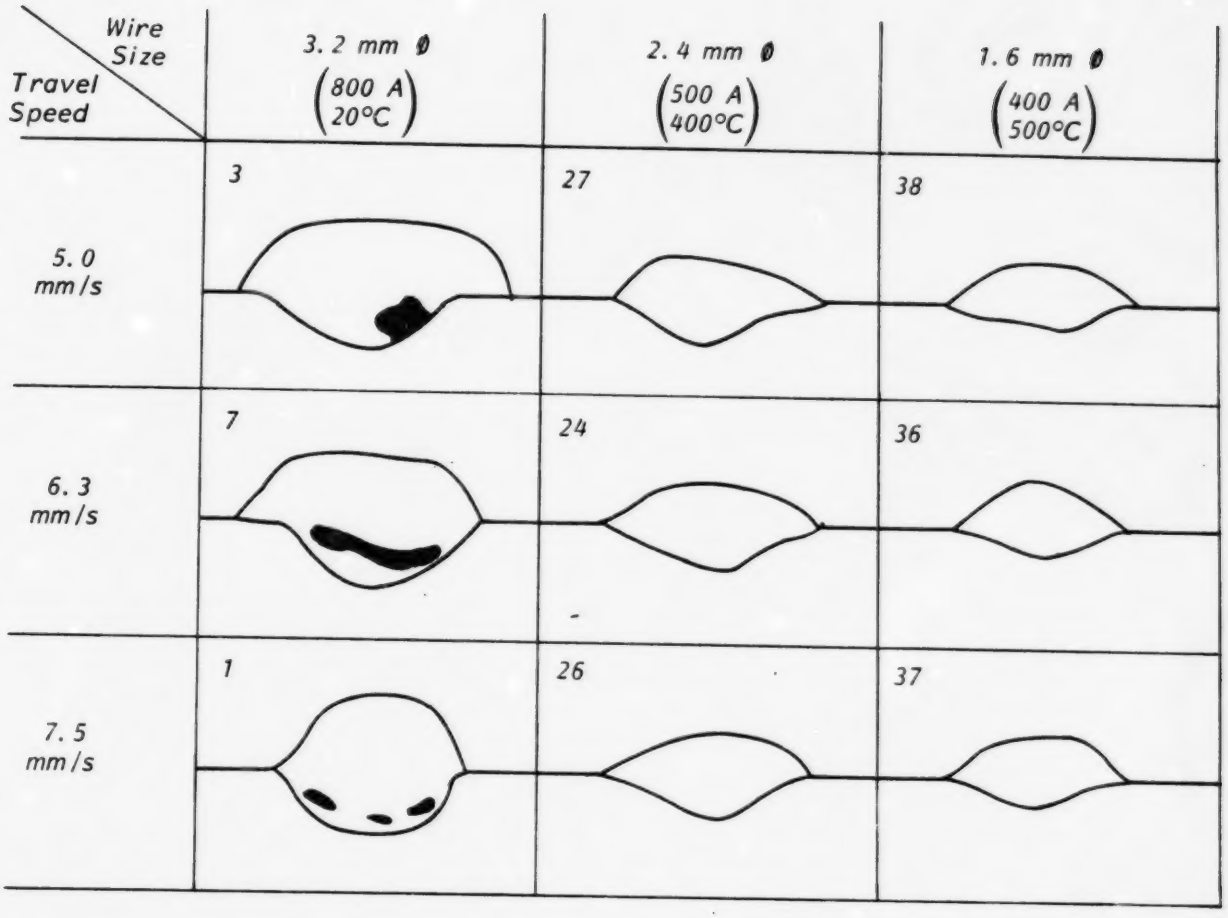

FIGURE 8
EFFECTS OF TRAVEL SPEED ON BEAD SHAPE

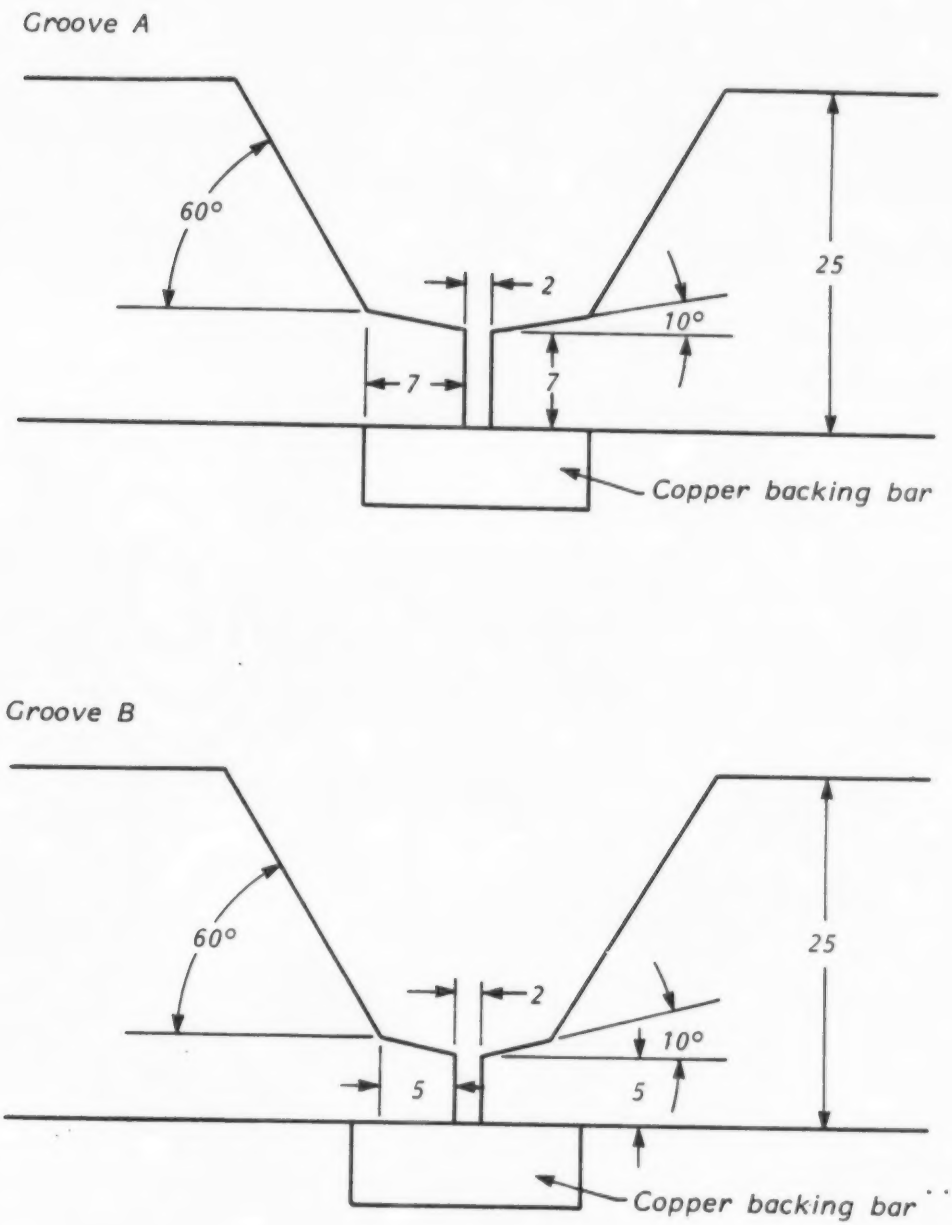

FIGURE 9
JOINT DESIGNS (BUTT WELDS)

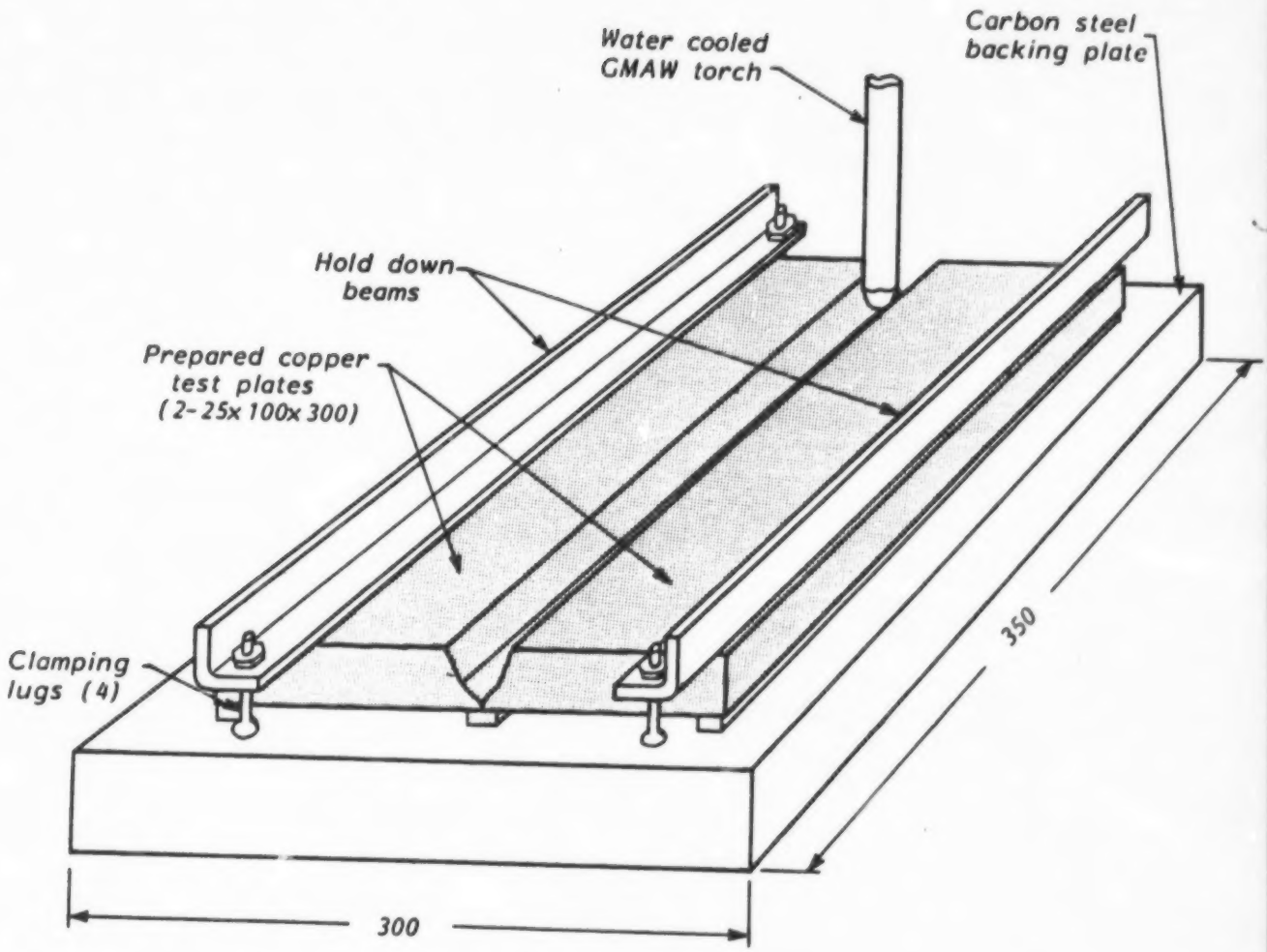

FIGURE 10
COPPER GMA GROOVE WELDING RESTRAINT JIG

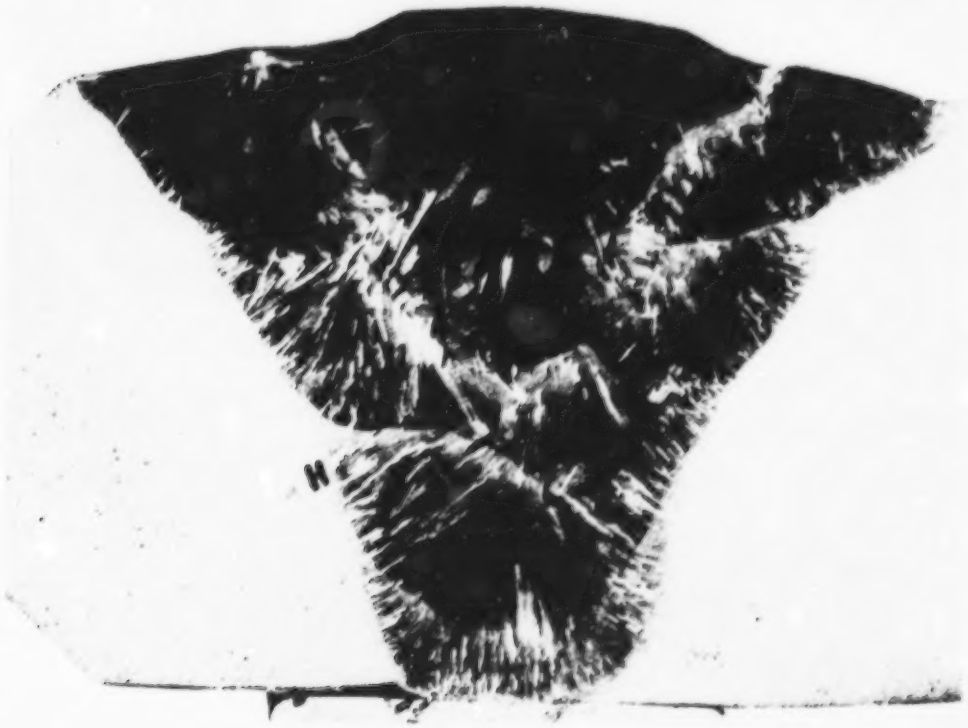

11a (Weld 43 - 3.5x)

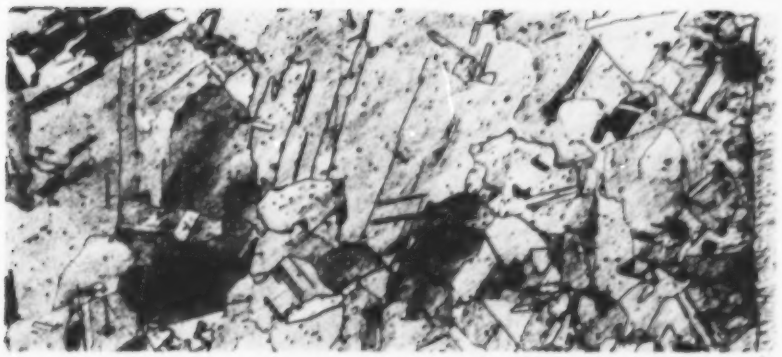

11b (from location 'H'-IIa)
Heat Affected Zone
from Fusion Line
(50x)

HAZ | Weld
Fusion Line

11c
Unaffected Base Metal
(ETP Copper) (50x)

FIGURE 11

170254 RD

MACROSTRUCTURE AND MICROSTRUCTURE OF A
TYPICAL ELECTROLYTIC TOUGH PITCH COPPER GMA WELD

FIGURE 12a (12.8x)
UNDERBEAD CRACKING

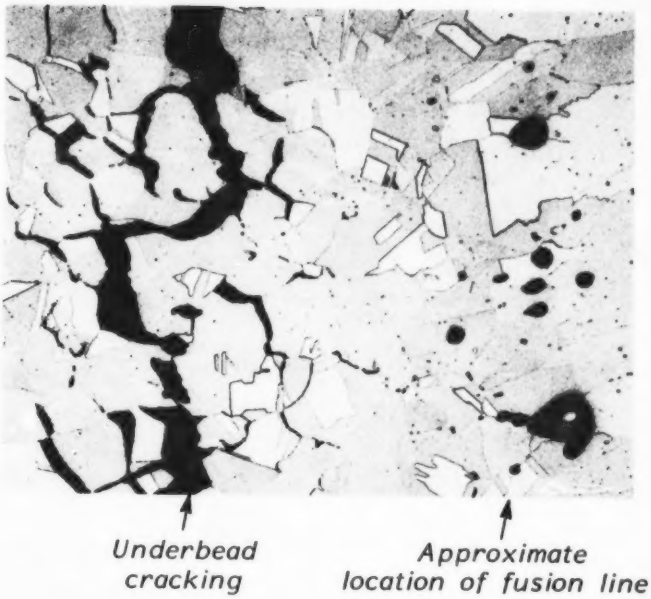

FIGURE 12b (160x)
UNDERBEAD CRACKING

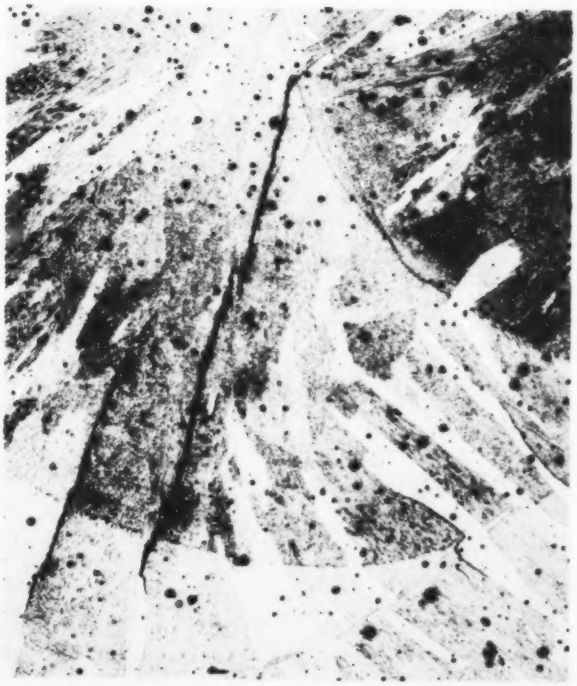

FIGURE 12c (12.8x)
CENTRELINE CRACKING

FIGURE 12
CRACKING FOUND IN WELD 15

FIGURE 13
WELD 22 (3.5x)

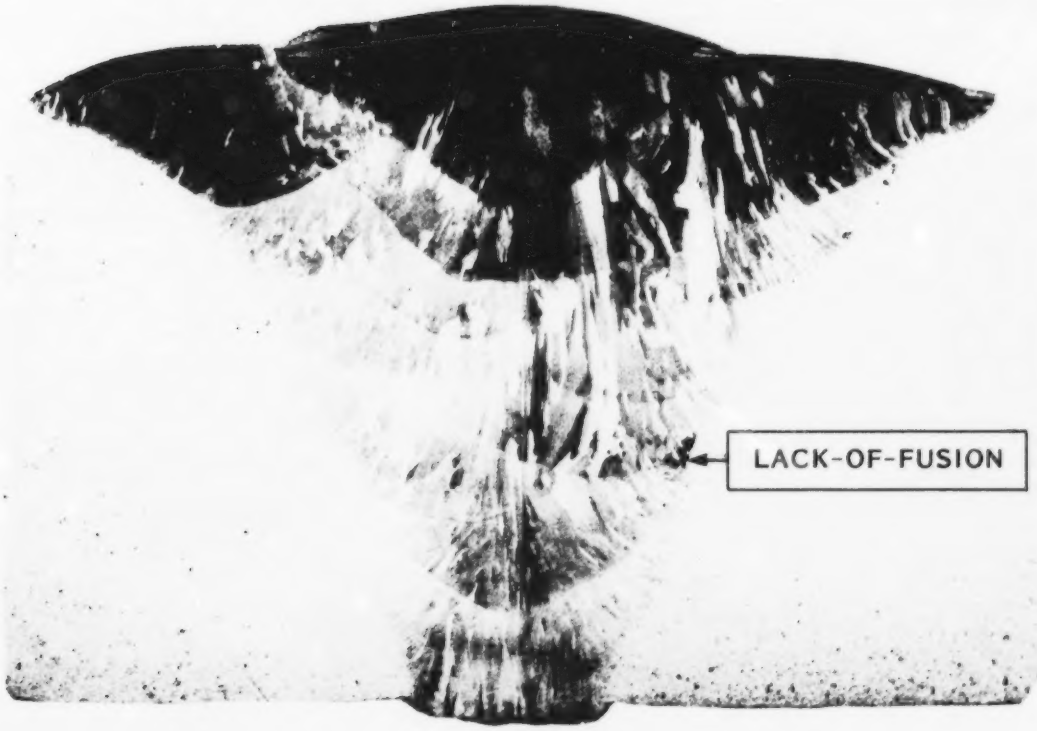

FIGURE 14
WELD 41 (3.5x)

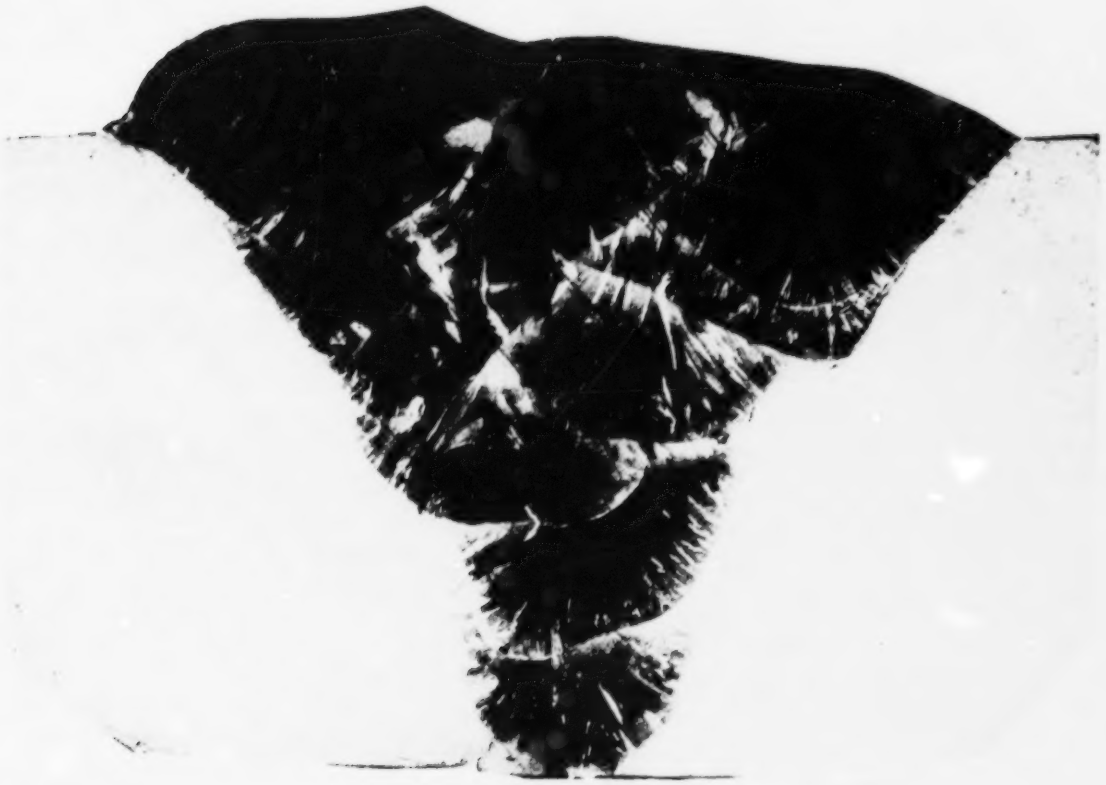

15a (3.5x)

15b (0.5x)

FIGURE 15
CROSS-SECTION AND RADIOGRAPH OF WELD 48
(200°C PREHEAT)

16a (3.5x)

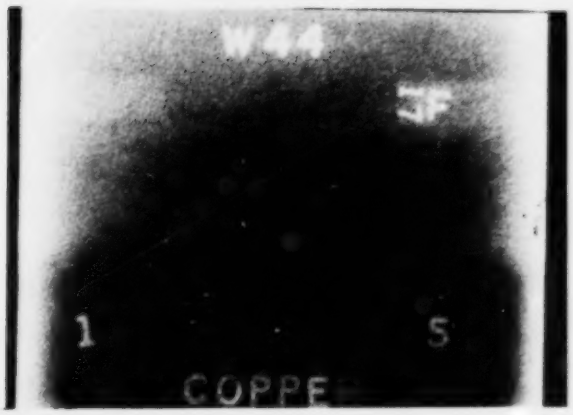

16b (0.5x)

FIGURE 16

CROSS-SECTION AND RADIOGRAPH OF WELD 44
(500°C PREHEAT)

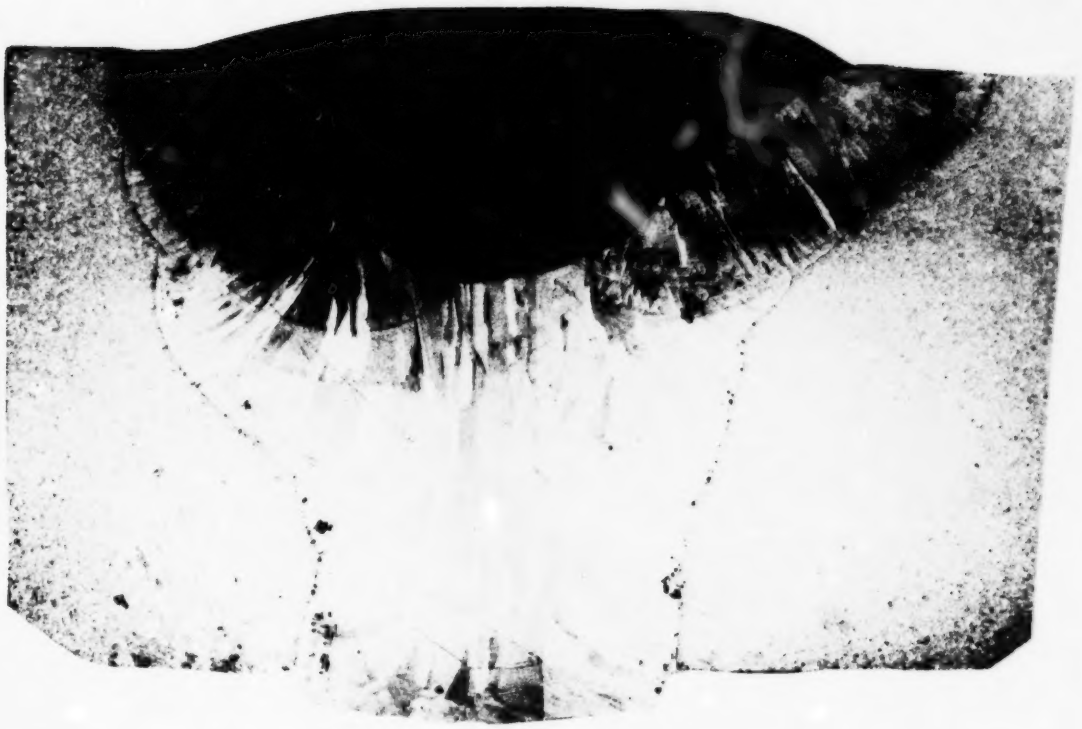

17a (3.5x)

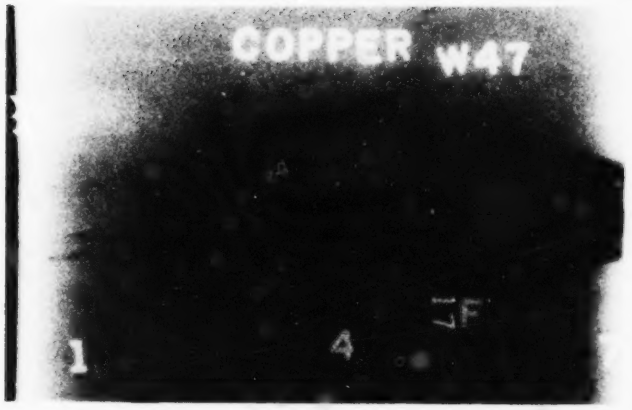

17b (0.5x)

FIGURE 17

CROSS-SECTION AND RADIOGRAPH OF WELD 47
(600°C PREHEAT)

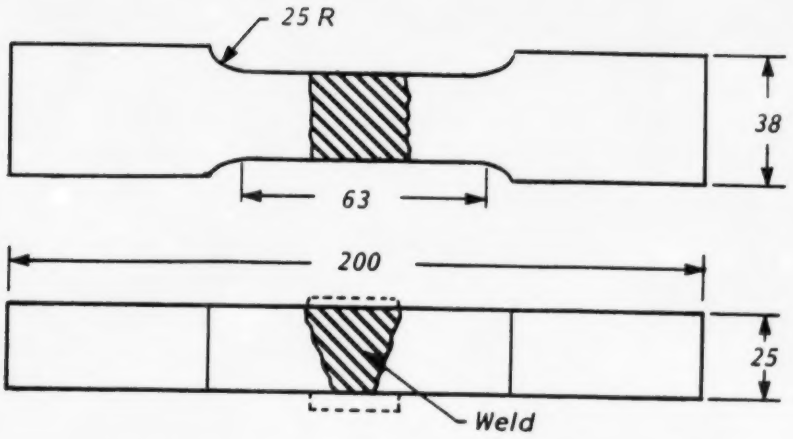

15(A) FULL SECTION TENSILE COUPON
(1/2 SCALE)

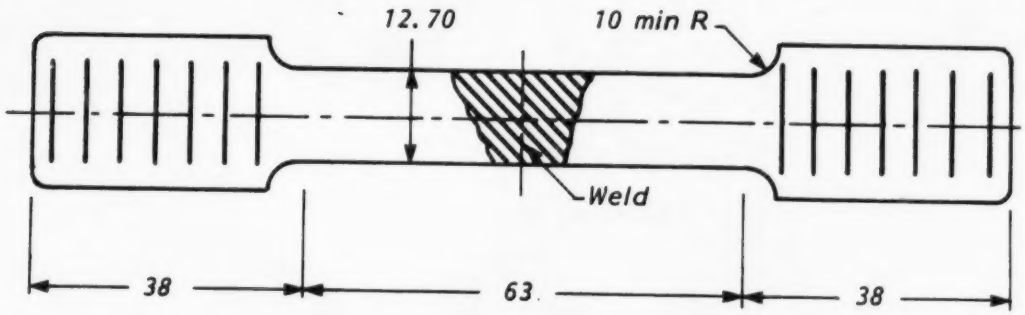

15(b) REDUCED SECTION (TURNED) TENSILE COUPON
(FULL SCALE)

FIGURE 18
COPPER WELD TENSILE TEST SPECIMENS
(DIMENSIONS IN mm)

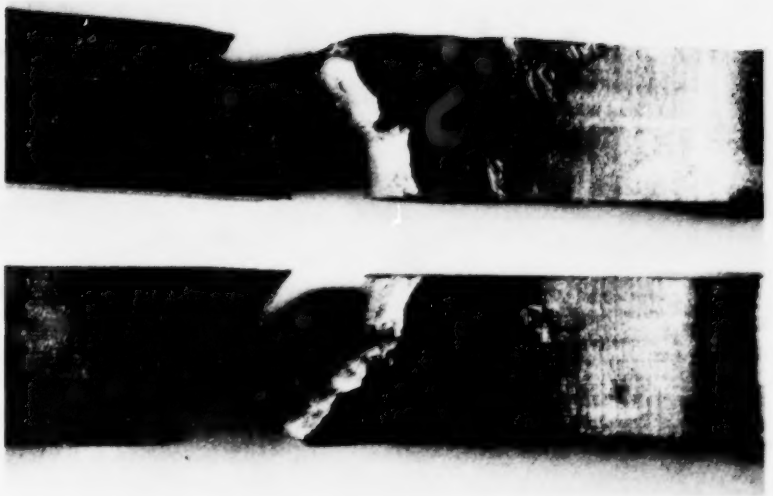

FIGURE 19

TENSILE TEST COUPONS SHOWING FRACTURE AT THE WELD METAL/BASE METAL INTERFACE (1.0x)

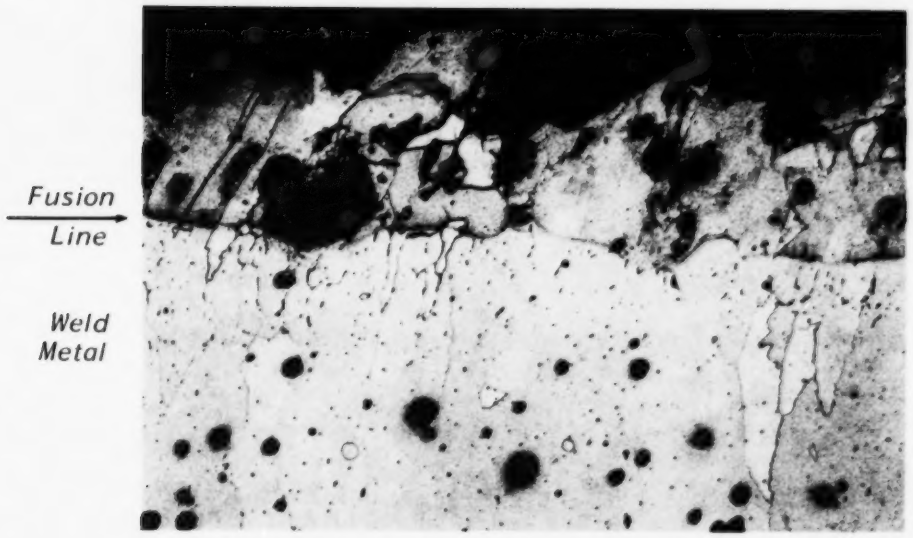

FIGURE 20

CROSS-SECTION THROUGH THE FRACTURE SURFACE OF TENSILE TEST COUPON 47b (100x)

FIGURE 21

TENSILE FRACTURE CROSS-SECTION THROUGH TENSILE TEST COUPON 44B (7x). FRACTURE IS IN THE WELD METAL
Note the Interdendritic Cracking

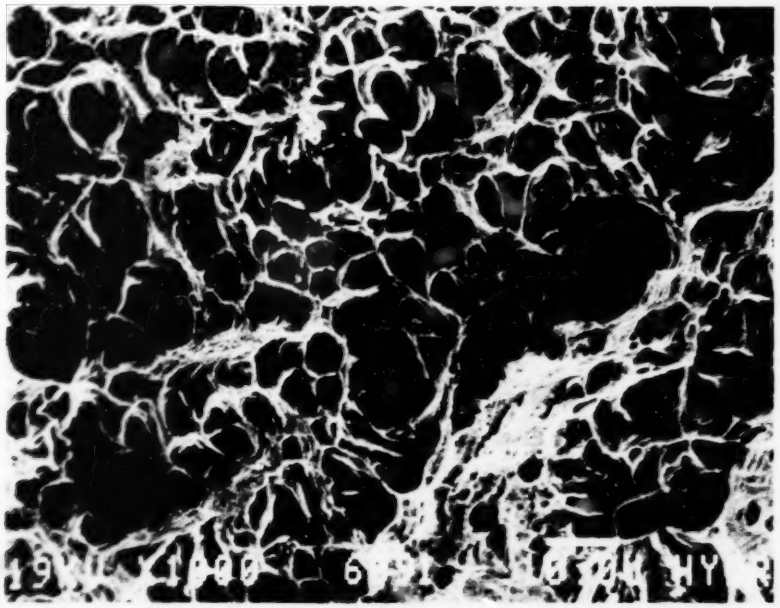

FIGURE 22

SEM FRACTOGRAPH OF TENSILE TEST COUPON 44B (1000x)
Note the Dimples in the Fracture Surface

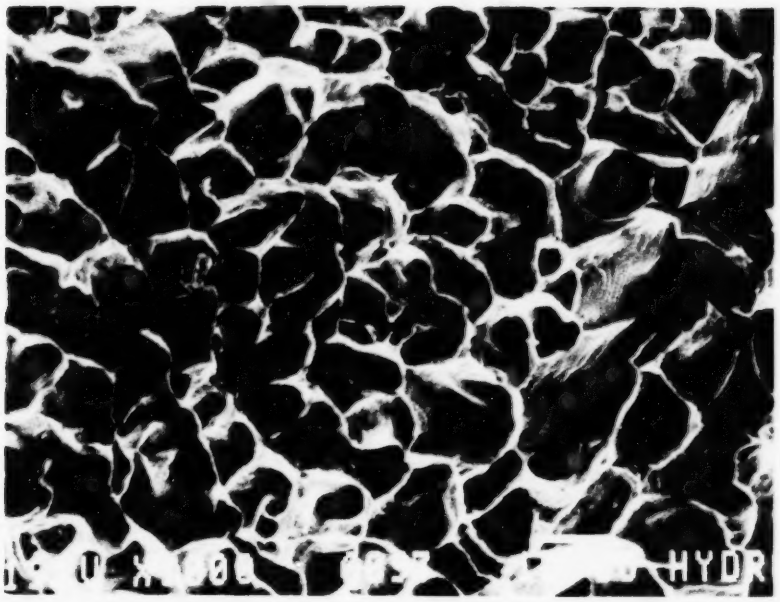

FIGURE 23

SEM FRACTOGRAPH OF TENSILE TEST COUPON 47A (1000x)
Note the Dimples in the Fracture Surface

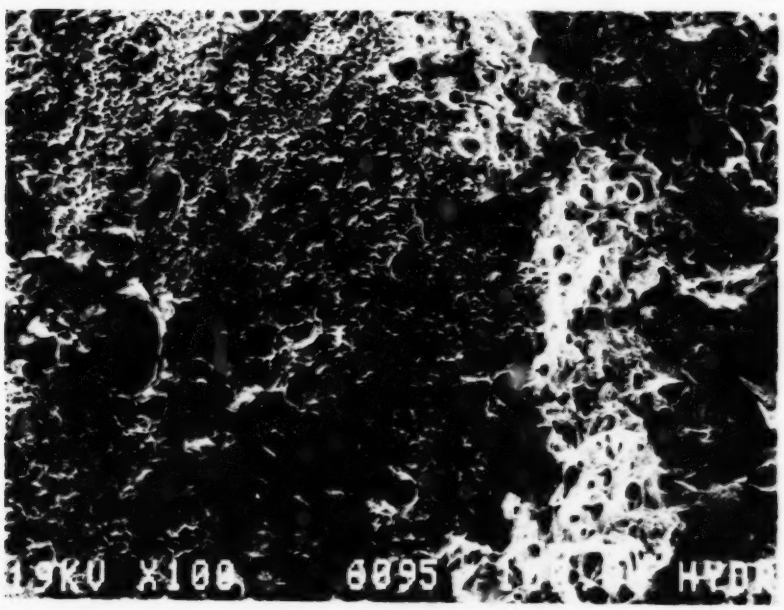

FIGURE 24

SEM FRACTOGRAPH OF TENSILE TEST COUPON 47A (100x)
Note the Presence of Gas Porosity in the Fracture Surface

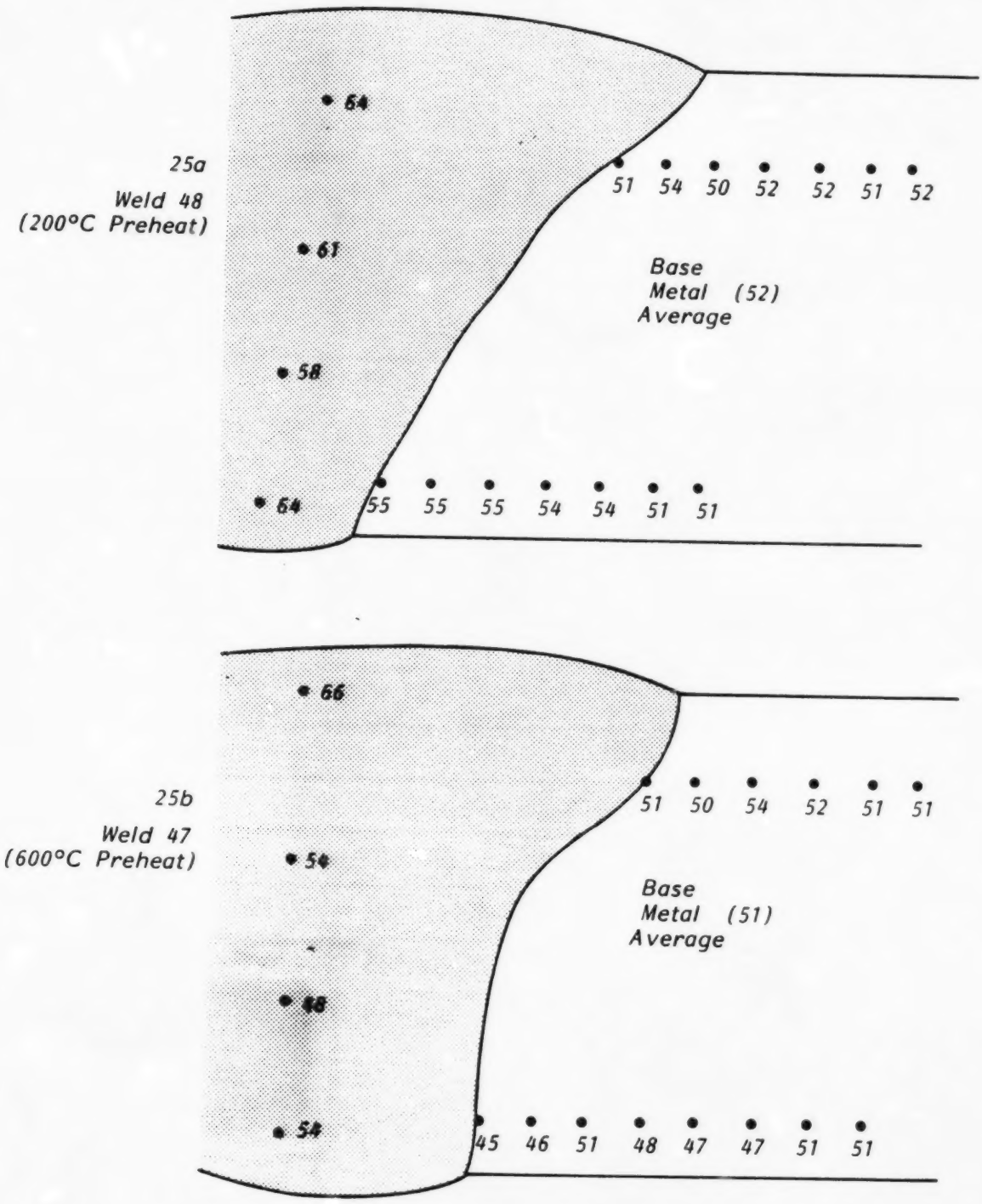

FIGURE 25

RESULTS FROM HARDNESS TESTING
(VICKERS - 1 Kg LOAD)

DISTRIBUTION

Mr. H.N. Isaac	Design & Development - Gen, H10A27
Dr. D. Mills	Director of Research
Mr. L. Crosthwaite	AECL, WNRE
Dr. K. Nuttall	AECL, WNRE
Mr. R.A. McEachran	Design & Development - Gen, H10A21
Mr. A.Y. Cheung	Design & Development - Gen, H14A25
Mr. M. Mikasinovic	Design & Development - Gen, H14B25
--Mr. J.T. Martin	Design & Development - Gen, H14A21
--Mr. G.S. Baichwal	Design & Development - Gen, H17A24
Mr. N. Hanssmann	Design & Development - Gen, H13F07
Mr. K. Sathi	Design & Development - Gen, H13F06
--Mr. G.G. Stephenson	Tech & Train Services, A8G2
Mr. J.W. Prince	Tech & Train Services, A8G8
--Dr. M.W. Shanahan	Tech & Train Services, A7H3
Mr. L.F. Robertson	Tech & Train Services, A7H6
Mr. J.H. Barbour	Hyd Gen & Trans, A5E2
Mr. J. McLaughlin	Bruce Heavy Water Plant
Mr. A. Kalnins	Darlington GS Const
Mr. J.A. Chadha	Mechanical Research
Mr. B. Teper	Mechanical Research
Dr. J. Brown	Metallurgical Research
Dr. M.D.C. Moles	Metallurgical Research
Dr. M.P. Dolby	Metallurgical Research
Dr. W.H.S. Lawson	Metallurgical Research
Mrs. S.V. Sandloehken	Metallurgical Research
Mr. M.J. Tinkler	Metallurgical Research
Mr. S.C. McNabb	Metallurgical Research
Mr. G. Poon	Metallurgical Research
Mr. P.Y.Y. Maak(4)	Metallurgical Research
Mr. J.G. Galloway(3)	Metallurgical Research

Public Reference Centre
Editorial Section(2)
Office Copies (3)
Extra Copies (3)

--Executive Summary Only

- last page -